Contract No:

This document was prepared in conjunction with work accomplished under Contract No. DE-AC09-08SR22470 with the U.S. Department of Energy (DOE) Office of Environmental Management (EM).

Disclaimer:

This work was prepared under an agreement with and funded by the U.S. Government. Neither the U. S. Government or its employees, nor any of its contractors, subcontractors or their employees, makes any express or implied:

1) warranty or assumes any legal liability for the accuracy, completeness, or for the use or results of such use of any information, product, or process disclosed; or
2) representation that such use or results of such use would not infringe privately owned rights; or
3) endorsement or recommendation of any specifically identified commercial product, process, or service.

Any views and opinions of authors expressed in this work do not necessarily state or reflect those of the United States Government, or its contractors, or subcontractors.

Hanford Double Shell Waste Tank Corrosion Studies- Final Report FY2020

Authors:

P. K. Shukla

R. E. Fuentes

B. J. Wiersma

DISCLAIMER

Hanford Double Shell Waste Tank Corrosion Studies- Final Report FY2020

P. K. Shukla
R. E. Fuentes
B. J. Wiersma

July 2021

Savannah River National Laboratory®

REVIEWS AND APPROVALS

AUTHORS:

_____ Date
P. K. Shukla, Materials Technology Division
Environmental and Legacy Management Directorate

_____ Date
R. E. Fuentes, Materials Technology Division
Environmental and Legacy Management Directorate

_____ Date
B. J. Wiersma, Materials Technology Division
Environmental and Legacy Management Directorate

TECHNICAL REVIEW:

_____ Date
J. T. Boerstler, Materials Technology Division, Reviewed per E7 2.60
Environmental and Legacy Management Directorate

APPROVAL:

_____ Date
J. Manna, Director, Materials Technology Division
Environmental and Legacy Management Directorate

_____ Date
J. S. Page, Tank and Pipeline Integrity
Washington River Protection Solutions

_____ Date
R. J. Nelson, Project Manager
Washington River Protection Solutions

ACKNOWLEDGEMENTS

EXECUTIVE SUMMARY

For fiscal year (FY) 2020, the Savannah River National Laboratory (SRNL) focused on three experimental tasks related to Hanford Double Shell Tank (DST) chemistry and integrity. The first task focused on understanding risk of corrosion due to formation of either continuous layers or discrete patches of deposits on the tanks' inner sidewalls and bottoms. The second task studied vapor space corrosion (VSC) of the secondary liner using two commercially available vapor corrosion inhibitors (VCIs) at manufacturer recommended dosages. Finally, the third task investigated the long-term open circuit potential (OCP) drift for mill-scale coupons, coupons with polished surfaces, and partial mill-scale coupons that were exposed to tank waste simulants. Additional tests were performed to evaluate the OCP drift as a function of the quantity and composition of organic compounds added to the simulant. A test that was included in the matrix that established the new chemistry limits for tank corrosion, but was previously unreported, was presented and reviewed as well.

1. New Limits

The conditions for the un-reported test, which was conducted in 2018, were described in previous reports [5] as Test 6 for the High Hydroxide Matrix. No nitrite was present in the solution. The Pitting Factor (PF) for this solution was 1.95, and since the minimum required PF was 1.2, it was anticipated that a cyclic potentiodynamic polarization (CPP) curve would produce a "pass" result. However, the CPP result was a mixed hysteresis "fail" with the appearance of small pits. To further assess this case, a potentiostatic test was performed. The potential was scanned from the OCP to a potential of 200 mV vs. saturated calomel electrode (SCE). The potential was held at this value for several hours so that pit propagation on the electrode surface could be assessed. After 25 hours a dramatic increase in the current density was observed, achieving a maximum of 1.43 mA/cm^2 before it settled at approximately 0.8 mA/cm^2 for 10 hours. After that time, the current decreased dramatically to a value between 20-80 µA/cm^2. This change in current is indicative of a decrease in the corrosion rate. The surface attack on the coupon was more typical of general corrosion than pitting corrosion. For the second test, 0.2 M nitrite was added to the solution, corresponding to an increase in the PF from 1.95 to 2.02. The CPP test in this solution resulted in negative hysteresis with no pits, corresponding to a pass. This means that the addition of nitrite of just 0.2 M for this dilute chemistry mitigated pitting corrosion. This test, in conjunction with other data from the test matrix, was instrumental in establishing the minimum limit for nitrite concentration as 0.2 M.

2. Underdeposit/Crevice Corrosion Studies

Modified AZ-101 simulant with a PF of 2 was used to evaluate the possibility of underdeposit corrosion on the tank bottom. The evaporated simulant salt was used as deposits. OLI simulations indicated that the salt deposits will include $NaF \cdot Na_2SO_4$ (Kogarkoite) that will persist and will not re-dissolve in the simulant. However, these deposits were not found to be adherent. As a result, the simulant chemistry above the deposits was able to percolate under the deposit and buffer any local chemistry under the deposits. This study indicated that presence of non-porous adherent deposits may be needed to initiate and propagate the underdeposit corrosion. Testing in FY21 will focus on the development of a non-porous adherent layer with representative sludge constituents.

3. Secondary Liner Corrosion Tests

VSC and immersion tests on rail-road car carbon steel samples were performed with the groundwater (GW) simulant at various dosages of VCIs. The VCIs tested were acquired from Cortec®.

- VCI-A: VpCI-337 – 10% v/v solution in GW simulant, i.e., 100 mL in VpCI-337 plus 900 mL of GW for 1 L VCI formulation.
- VCI-B: 10% wt. VpCI-609 in GW simulant (100 g VpCI-609 in 1 L) and 0.75% v/v VpCI-649MF (7.5 mL/L)

VCIs formulations were added after 2 months of exposure. The tests on the corroded coupons were continued for an additional 4 months. Three tests were conducted using VCI-A and VCI-B. The first two tests were conducted using 100% recommended dosages of VCI-A and VCI-B. The third test was conducted at 50% of the recommended dosage of VCI-B. The following conclusions are made from the experimental data and results:

- Both VCIs were effective in mitigating the pitting corrosion rate for carbon steel coupons immersed in groundwater and at heights up to 18 inches above the liquid surface for the 100% recommended dosages. VCI-B was more effective than VCI-A in mitigating the pitting corrosion rate at heights up to 36 inches above the liquid level. On the other hand, a statistical analysis of the pitting corrosion rate data suggested that VCI-A may not have significantly reduced the pitting corrosion rate at the 36 inch level and therefore would not be as effective as VCI-B.
- 50% VCI-B was also effective in mitigating the pitting corrosion rate for coupons that were immersed and at a height 6 inches above the liquid surface. However, a statistical analysis of the pitting corrosion rate data indicated that it was not as effective in mitigating corrosion of the coupons that were 18 inches or higher above the liquid surface.
- 100% VCI-B was also effective in mitigating the surface average corrosion rate for the coupons immersed in groundwater and at heights up to 18 inches above the liquid surface. VCI-A was only effective in reducing the surface average corrosion rate for the coupons immersed in the groundwater. 50% VCI-B was effective in mitigating the surface average corrosion rate for the immersed coupons and at heights up to 6 inches above the liquid surface.

4. Long term OCP Drift Tests

Evolution of the OCP was studied for three tank waste simulants identified as AY-101, SY-101, and AW-105. In addition, OCP evolution tests in two variants of the AW-105 chemistry were performed. Both variants contained limited quantities of normal paraffin hydrocarbons (NPH) and additions of tributylphosphates (TBP). The difference between the variants was that two different concentration levels for the tributylphosphates were utilized. Coupons with three different surface conditions were used. The surface conditions included polished, mill-scale, and partial mill-scale.

The results of the final potentials measured in each simulant are summarized in Table E-1. The OCP of the coupons with the three different conditions evolved to the same value in AY-101 simulant and appeared to reach a steady state at -140 mV$_{SCE}$ after approximately 600 hours. These values were slightly more cathodic than that observed for the initial in-tank measurement for Tank AY-101 (-77 mV$_{SCE}$). The coupons' OCP in SY-101 differed by as much as 250 mV, depending on the surface condition, and continued to evolve even after 4000 hours of exposure. The OCP measured from the mill-scale coupon was closest to the tank wall potential (i.e., OCP for mill scale sample was -298 mV$_{SCE}$, while the tank wall OCP is -257 ± 13 mV$_{SCE}$). The OCP of the coupons in AW-105 Base (without NPH and TBP) were in the range of -200 to -300 mV$_{SCE}$ after 4000 hours of exposure. Similarly, corrosion potentials for the coupons immersed in AW-105 Representative (with NPH and TBP) also ranged between -200 to -300 mV$_{SCE}$ after 2100 hours of exposure. These values are close to the in-tank potentials measured in AW-105 during the initial probe readings. The OCP for the coupons immersed in AW-105 Elevated TOC (with elevated NPH and TBP) were in the range of -450 to -600 mV$_{SCE}$ after 4000 hours of exposure. The lower potential readings were likely the response to the increase in organic concentrations for this last variant.

The OCP observations were mostly consistent with previous laboratory results. Anodic OCP drift was observed initially in all cases. An unexplained cathodic shift in the potential for the mill scale and partial mill-scale tests after approximately 2500 hours in SY-101 occurred. The same trend was observed for the partial mill-scale tests in the AW-105 Base. However, these values actually ended up being similar to the in-tank measurements that were made. The final potential appears to be dependent on the hydroxide concentration (i.e., higher hydroxide concentrations result in more negative OCP values). Finally, the presence of organics in sufficient quantities also results in more negative OCP values.

Table E-1 Summary of Final OCP (mV_{SCE}) Data in Waste Simulants

Simulant	Bullet		Mill-Scale		Partial Mill-Scale	
	Initial	After	Initial	After	Initial	After
AY-101	-557	-140	-175	-140	-388	-140
SY-101	-492	-73	-183	-304	-324	-333
AW-105 with small-chain organic acids (i.e., formate, acetate, glycolate) or AW-105 Base	-668	-256	-284	-201	-405	-319
AW-105 with small-chain organic acids, the TBP family of organics, and NPH organics or AW-105 Representative	-516	-236	-205	-240	–	–
AW-105 with small-chain organic acids, elevated concentrations of the TBP family of organics, and NPH organics or AW-105 Elevated TOC	-893	-461	-300	-435	-299	-573

Following the OCP test, electrochemical impedance spectroscopy (EIS) and CPP data were collected for each material condition and simulant. The CPP data for the three coupon types in the five simulants, exhibited category 1 behavior, i.e., pitting corrosion of the tank steel is unlikely in these simulants. However, the passive current density of the mill-scale and partial mill-scale coupons was one to two orders of magnitude higher than the bullet coupons in all five simulant chemistries. A similar trend was observed in the EIS data of the three coupon types in the five simulants. The low frequency impedance of the mill-scale and partial mill-scale coupons were lower than the bullet coupons impedance. The EIS and CPP data are cross-consistent, i.e., evidence of bullet coupons' lower passive current density compared to mill-scale and partial mill-scale coupons in the CPP current is exhibited in form of higher impedances of the bullet coupons compared to the other two coupon types. There are two plausible explanations for the higher passive current densities of the mill-scale and partial mill-scale coupons compared to the bullet coupons: (i) there are anodic reactions other than the metal dissolution reactions that occur on the mill-scale and partial mill-scale coupons leading to higher current densities during the forward scans of the CPP curves, and (ii) the passive film that develops on the exposed metal surface of the mill-scale and partial mill-scale coupons could not be fully developed due to the presence of the oxides. These two hypotheses require further investigation.

TABLE OF CONTENTS

LIST OF TABLES

LIST OF FIGURES

LIST OF ABBREVIATIONS

ASTM	American Society for Testing and Materials
CPP	Cyclic Potentiodynamic Polarization
DNV-GL	Det Norske Veritas-Germanischer Lloyd
DST	Double-Shell tank
EDM	Electrical Discharge Machine
ER	Electrical Resistance
FY	Fiscal Year
GW	Ground Water
LCM	Laser Confocal Microscope
LDP	Leak Detection Pit
MIC	Microbiologically Influenced Corrosion
mpy	mils per year
NDE	Non-Destructive Examination
NPH	Normal Paraffin Hydrocarbon
OCP	Open Circuit Potential
PF	Pitting Factor
PTFE	Polytetrafluoroethylene
SCC	Stress Corrosion Cracking
SCE	Saturated Calomel Electrode
SRNL	Savannah River National Laboratory
SST	Single-Shell Tank
TAPI	Tank and Pipeline Integrity
TBP	Tributyl Phosphate
TIEP-CSG	Tank Integrity Expert Panel-Corrosion Sub-Group
TOC	Total Organic Carbon
VCI	Vapor Corrosion Inhibitor
VSC	Vapor Space Corrosion
WRPS	Washington River Protection Solutions
WTP	Waste Treatment and Immobilization Plant

1.0 Introduction

The Hanford Site in Washington State has millions of gallons of legacy radioactive waste that is being retrieved from single shell tanks (SSTs) and transferred to newer double shell tanks (DSTs) for eventual closure of SSTs. The waste will be maintained in DSTs until eventual immobilization can be performed at the Waste Treatment and Immobilization Plant (WTP), currently under construction. A detailed integrity program plan, implemented by Washington River Protection Solutions (WRPS) Tank and Pipeline Integrity (TAPI) organization, has been developed for the DSTs, which has many elements including waste chemistry control for corrosion mitigation, visual inspections and non-destructive examination (NDE) of tank walls.

Corrosion testing for DSTs has been directed by the Tank Integrity Expert Panel-Corrosion Sub-Group (TIEP-CSG) to provide the technical guidelines for the corrosion control program. Corrosion testing has been performed at three independent laboratories: Det Norske Veritas-Germanischer Lloyd (DNV-GL), Savannah River National Laboratory (SRNL), and the 222-S facility at Hanford operated by WRPS. SRNL has focused its corrosion studies on vapor space corrosion (VSC), development of corrosion chemistry limits to mitigate pitting corrosion, and corrosion protection for the DST secondary liner.

Recently, SRNL has been instrumental in developing a new approach to waste chemistry control [1]. SRNL continues to provide support for the refinement and implementation of these new limits for the DSTs. SRNL is also addressing the observation of accelerated attack of the exterior of the annulus floor observed in the DSTs. To investigate this matter, experiments for VSC were performed to establish vapor corrosion inhibitors (VCIs) effectiveness after coupons have been exposed to ground water. Long-term potential drift studies have been performed to investigate the environmental and material surface parameters that influence final steady state potential that is achieved.

For fiscal year (FY) 2020, SRNL focused on three experimental tasks. The first task focused on understanding risk of corrosion due to formation of either continuous layers or discrete patches of solids on the tanks' inner sidewalls and bottoms. The second task focused on VSC studies for the secondary liner using two commercially available VCIs at manufacturer recommended dosages. The VCI formulation was applied at the mid-point of the experiment to determine its performance on weathered coupons. Finally, the third task was dedicated to the study of long-term open circuit potential (OCP) drift for three waste tank simulants. These tanks currently have reference electrodes installed for monitoring the OCP. A comparison between the laboratory results and the tank potentials was made. Additionally, different quantities of organics were added to one of the waste simulants to study their effects on the measured OCP.

2.0 Background

DST corrosion testing for FY20 enumerated six tasks activities [2]. From the six task activities, only three were based on experimental studies performed at SRNL. A background is provided below for these three tasks.

2.1 Underdeposit/Crevice Corrosion Studies

Formation of saltcake and scale-like deposits on the wall and the bottom of several Hanford DSTs have been observed; this is based on the loose, small particulate solids in core samples taken from the tanks and post retrieval inspection of the inner surface of the primary tank of AY-102. These solids may promote underdeposit corrosion, which occurs when the liquid above the solids, seeps in between the solids and the metal surface. This crevice condition may create an aggressive local environment that becomes very

corrosive to the metal. The overall objective of this task was to determine the effect of solid deposits on the corrosion risk to the tank bottom, and whether a combination of scale, saltcake and loose solids lead to underdeposit corrosion. These results will be compared to the results of a corrosion test performed in a liquid sample of the same composition with no deposits present.

2.2 Secondary Liner Corrosion

There are 27 active DSTs at the Hanford Site. Each DST consists of a primary liner (inner) surrounded by a secondary (outer) liner. The secondary liner rests on a concrete pad. A schematic diagram presented in Figure 2-1 for some DSTs (e.g., AY, AZ and SY Tank Farms), shows the concrete foundation and drain slots.
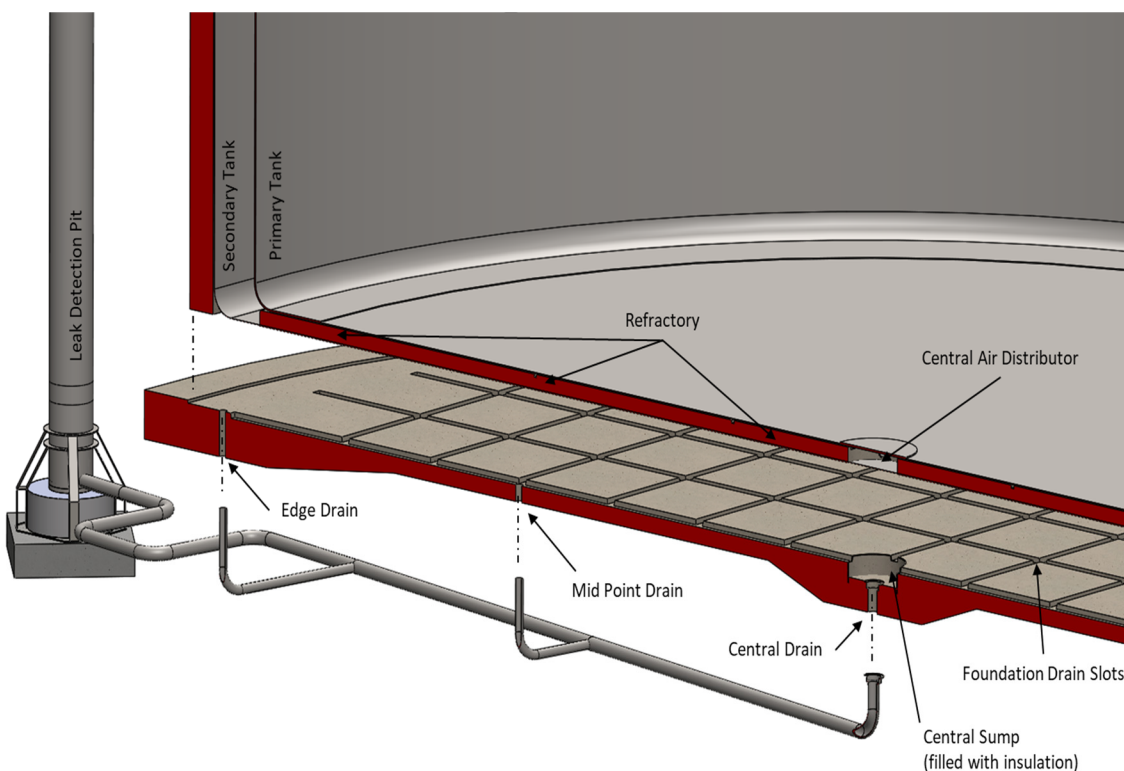
Figure 2-1 Schematic of a double shell tank depicting primary and secondary tank shells, concrete foundation, and drain slots.

Water is known to accumulate in the drain slots and may cause corrosion on the exterior of the secondary liner. Ultrasonic inspection is confined to the annular space between the primary and secondary tanks, leaving a concern that corrosion is widespread on the underside of the secondary liner bottom plate. Since the water level can vary in the drain slots based on accumulation, corrosion could be caused by direct contact with the accumulated water, or when the water level is below the underside of the tank bottom, VSC could also occur. Accumulated water is drained through the sumps into Leak Detection Pits (LDPs). The drained water was analyzed for its constituents, and two simulants were developed considering the chemical composition range of the accumulated water. The simulants were identified as LDP water and ground water (GW).

Testing with LDP and GW simulants for legacy carbon steel corrosion was started in FY14 with a long-term immersion experiment in which the deleterious effects of these chemistries were observed, with mass loss corrosion rates obtained of approximately 10 mils per year (mpy) [3],[4]. During FY16 testing was

focused on the inhibition strategies using commercial VCI to coat the samples and minimize VSC and other types of corrosion. Testing continued during FY17, and it was observed that by coating the samples with VCI, the corrosion inhibition was short-lived and did not significantly reduce carbon steel corrosion [5].

To investigate corrosion control measures for the secondary liner, a vapor corrosion inhibitors (VCIs) from Cortec® (VpCI-337, VpCI-609, and VpCI 645) were acquired in FY 2018. Experimental studies were conducted by directly adding the corrosion inhibitors to the groundwater solution. The inhibition towards carbon steel was monitored for VSC using electrical resistance probe and tested during a four-month immersion test.

For FY19, VCIs from Cortec® (VpCI-337, VpCI-609, and VpCI 649MF) were investigated. SRNL performed experiments with the ground water simulant which will be inhibited after corrosion on exposed coupon has initiated and propagated, i.e., weathered or pre-corroded coupons. The use of pre-corroded coupons was used to determine whether VCIs are effective in mitigating corrosion on steel surface that has already experienced extensive corrosion and is covered with pre-existing corrosion products. In addition, an experiment was conducted below the manufacturer recommended dosage. VCIs were added to a simulated groundwater solution during mid-course of experiments (i.e., after corrosion has been initiated in most coupons). The inhibition towards carbon steel was monitored for VSC using electrical resistance probes and tested during a six-month immersion test. The data suggested that VCIs are able to mitigate corrosion on the weathered coupons when dosed at the vendor recommended levels, and also at 50% of the recommended levels. For this task in FY20, the objective was to find the VCI strategies that can effectively minimize corrosion of carbon steel exposed to GW.

2.3 Long-Term OCP Drift

Approximately 55 million gallons of radioactive waste is being stored in 177 carbon steel tanks at Hanford. Long-term performance and integrity of the tanks is partly dependent on modifying the waste chemistry such that risk of pitting and SCC of the tank carbon steel are mitigated. To this end, CPP experiments were conducted to identify risk of pitting corrosion, and subsequently determine the level of inhibition needed to mitigate pitting corrosion in the DSTs. One of the key parameters associated with the determination is the difference between the corrosion and repassivation potentials: if the corrosion potential is greater than repassivation potential, the risk of pitting corrosion exists.

It has been observed that certain simulated waste chemistries lead to significant changes in OCP over time [7], [9]. A distinction is drawn between OCP and corrosion potential. At the corrosion potential, rates of anodic and cathodic reactions balance each other, and the metal surface is in steady equilibrium with the surrounding electrolyte. OCP is defined as the measured potential as the metal surface is in the process of establishing equilibrium with the surrounding electrolyte. The rates of anodic and cathodic reactions are evolving as well, even though the reactions' rates balance each other during the evolution. When the evolution reaches a steady-state (i.e., potential does not change more than +/- 10 mV/hr), OCP becomes the corrosion potential of a metal surface in a given electrolyte. The change in OCP during CPP tests could lead to underassessment of the risk especially when corrosion potential is below the repassivation potential and the difference between the two is sufficiently low such that an upward drift in OCP would increase the risk of the corrosion potential exceeding the repassivation potential, thereby, increasing the risk of localized corrosion in the form of pitting corrosion. Therefore, to quantify the risk of pitting corrosion due to OCP drift, laboratory experiments were conducted with three waste simulant chemistries with pre-determined repassivation potentials in the CPP data.

Another key difference between laboratory testing using CPP and field conditions has been the surface condition of coupons used in the laboratory testing in comparison with the field condition of the tanks. CPP

tests have been conducted using bullet coupons with 600-grit polished surfaces, whereas the tanks were constructed using steel with mill scale plus corrosion products. It is recognized that during the construction process, large sheets of the carbon steel were welded together, and other processes associated with tank construction likely would have disturbed the original mill-scale on portions of the tank liner. Considering this, a 600-grit polished coupon was utilized as one extreme of the surface condition, whereas a coupon with mill-scale plus corrosion products is considered the other extreme. The surface condition of a newly constructed tank is expected to be somewhere between the two extremes. In addition, the tanks were put in service sometime after completion of construction. This would have resulted in the tank steel being exposed to ambient conditions, which included raw water utilized for hydrostatic testing, and developing additional layers of corrosion products before being placed in service. Considering several possibilities of the surface conditions, the study also included examining the effect of surface condition on the evolution of OCP. The objective also included establishing conservatism of the CPP tests results, i.e., the test results sufficiently bound the conclusions derived from the test data.

3.0 Task Description and Activities

The tasks and activities that were performed during FY20 are listed and described in the sections below.

3.1 Task 1: Completion of FY19 report

Task 1 was the completion of the FY19 report for worked performed during that FY. The report was completed and issued on July 2020 [7]. It included work on New Limits, Secondary Liner corrosion testing using VCIs, Long-term OCP drift studies and Microbiologically induced corrosion (MIC) of ground water samples.

3.2 Task 2: New Chemistry Control Limits Implementation and Technical Support

New chemistry control limits for the DST wastes were recommended in FY19 [1]. For this report, a test result that was not provided in previous reports is presented. The test result, in conjunction with other tests in the matrix, provides the basis for the minimum nitrite concentration of 0.2 M.

3.3 Task 3: Crevice/Underdeposit Corrosion Beneath Tank Bottom Solids

Loose, small, insoluble solids have been observed in the core samples taken from DSTs (e.g., AZ-101). These solids may lead to underdeposit corrosion, a form of crevice corrosion, which is aggressive on carbon steel. The overall approach involved using Tank AZ-101 interstitial liquid simulant to assess the risk of corrosion of the tank steel, with and without presence of solids. The pitting factor for AZ-101 interstitial liquid is approximately 4 as determined by the Best Basis Inventory [8]. The hydroxide concentration was adjusted to lower the pitting factor in the 1-2 range to account for uncertainties in the characterization and to address potential worst case concentrations that could evolve over time beneath the deposit. Four tests were conducted at 70 °C with the following exposure conditions: (i) tank steel without deposits, (ii) tank steel with saltcake as solid deposits spread throughout coupon surface, (iii) saltcake deposits localized to small area of a coupon surface, and (iv) tank steel with saltcake and solids that mimic the core sample and localized to small area on coupon surface.

3.4 <u>Task 4: Secondary Liner Corrosion Testing</u>

FY20 studies were conducted with commercially available VCIs at manufacturer recommended dosages, identified in this report as VCI-A and VCI-B. Three tests were conducted with carbon steel coupons exposed to a GW environment. For two of the tests, each VCI was tested separately at 100% of the recommended dosage. The third test was conducted at 50% of the recommended dosage of VCI-B. Prior studies with VCIs have shown that VCIs' effectiveness vanish at 10% of the recommended dosages for the aboveground tank bottom underside applications [9]. Therefore, to determine a lower limit of effective VCI dosage, 50% of the recommended dosage was used to determine minimum VCI concentration needed for the secondary liner application. All three tests were conducted with twenty-four coupons for each experiment. Of these, six coupons were immersed, and the remaining eighteen coupons were placed in the vapor space of the vessel. Twelve coupons were extracted from each experiment after 2 months. VCIs were added to the test solutions in each experiment at the time of extraction of the first twelve coupons. The remaining coupons were extracted after being exposed to the VCI treated solutions for an additional four months. The coupons were analyzed for both pitting and general corrosion rates. The corrosion rate data were used to determine performance of the VCIs on the weathered coupons and the effect of lower than recommended VCI dosages on corrosion mitigation. Electrical Resistance (ER) probes were also used for in-situ measurement of corrosion rates and VCI performance. ER probes were immersed in the electrolyte and also positioned near the liquid and vapor space interface. ER probe data were continuously collected and analyzed to in-situ measure the corrosion mitigation performance of the VCI treated solutions.

3.5 <u>Task 5: Long-Term OCP Drift Corrosion Testing</u>

Laboratory experiments were conducted to determine the source(s) of OCP drift. This could help determine how to best interpret reference electrode data that is being collected in the Hanford tanks. Three simulant chemistries representative of Tanks AY-101, SY-101, and AW-105 were selected for FY20. The simulant chemistry for AW-105 was further varied to investigate the effects of the organic constituents on the OCP evolution and steady-state corrosion potential. For AW-105, three variations of the simulant were used: AW-105 with small-chain organic acids, AW-105 with small-chain organic acids along with representative NPH and TBP concentrations and AW-105 with small-chain organic acids and higher concentrations of NPH and TBP.

The OCP was measured along with the corrosion current density and polarization resistance data. The tests were conducted at 35 °C. Each test contained three electrodes: (i) 600-grit polished coupon, (ii) mill-scale plus corrosion products, and (iii) partial coverage of mill-scale plus corrosion products. OCPs of the six coupons in each simulant chemistry were monitored over a period of several months. Electrochemical impedance spectroscopy (EIS) measurements were conducted after the OCP measurements, followed finally by CPP measurements. The corrosion potential, EIS and CPP data were used to determine changes in pitting corrosion risk due to evolution of corrosion potential and electrochemical properties of the metal surface.

4.0 Experimental Procedure

The material used for all corrosion testing was carbon steel selected from AAR TC-128 Rail Car Steel. This steel was selected for testing since it approximates the chemistry and microstructure of American Society for Testing and Materials (ASTM) A515, Grade 60 carbon steel, the steel from which some of the DSTs were fabricated [10]. The chemical composition of the steel is shown in Table 4-1.

Table 4-1 Chemical Composition of AAR TC-128 Rail Car Steel

	C	Mn	P	S	Si	Fe
Specification (wt.%)	0.24 (max.)	0.9 (max.)	0.035 (max.)	0.04 (max.)	0.13 to 0.33	Balance
Measured (wt.%)	0.212	1.029	0.012	0.013	0.061	Balance

Described next are the experimental details and conditions in which the carbon steel was used and prepared for the secondary liner corrosion testing.

4.1 Underdeposit Corrosion Testing

The underdeposit corrosion testing was conducted using AZ-101 simulant. The simulant composition is provided in Table 4-2. The PF for the AZ-101 waste samples are close to 4; hence the hydroxide concentration in the waste chemistry was adjusted to obtain a pitting factor of two in order to investigate a more aggressive chemistry.

The experiments were conducted with 3-inch diameter × 0.25-inch thick coupons made of the rail car carbon steel whose chemical composition is listed in Table 4-1. The deposits were formed on the coupons by evaporating the simulant. A total of four tests were conducted. Details of each test are listed in Table 4-3. All four tests were conducted at 70 °C and atmospheric pressure, with the duration being four months for all four tests.

Table 4-2 Chemical Composition of AZ-101 Simulant

Source Chemical	Concentration (M)
Sodium hydroxide	0.0818
propionic acid	0.00075
Sodium aluminate	0.025
Sodium fluoride	0.120
Sodium nitrite	1.60
Sodium nitrate	0.826
Potassium nitrate	0.12
Trisodium phosphate, 12-hydrate	0.020
Sodium sulfate	0.050
Sodium carbonate	0.570
Sodium chromate	1.00E-03
Boric acid	1.00E-03

Table 4-3 Test Matrix for Underdeposit/Crevice Corrosion

Experiment Identification	Deposit Condition	Notes
Experiment 1 (Control)	None	The control experiment was conducted with the AZ-101 simulant listed in Table 4-2, without any deposits.
Experiment 2 (Deposits covering entire coupon surface)	250 mL of the AZ-101 simulant was evaporated to form deposits. Deposits covered entire surface of the coupon.	Simulant solution was added to the test setup after deposition of the solid on the coupon's surface.
Experiment 3 (Deposits covering limited area of the coupon surface)	Deposits formed by evaporation of the AZ-101 simulant were localized to a one-inch diameter area on the 3-inch diameter coupon surface.	Simulant solution was added to the test setup after deposition of the solid on the coupon's surface.
Experiment 4 (Deposits formed by AZ-101 evaporates and kaolin, deposits covered limited area of the coupon surface)	Deposits formed by evaporation of the AZ-101 simulant were mixed with kaolin. Deposits were focused on one-inch diameter disk on the 3-inch diameter coupon surface.	Simulant solution was added to the test setup after deposition of the solid on the coupon's surface.

Regarding Experiments 3 and 4, an approximately 1-inch diameter glass ring was attached with silicone on the two mounted coupons. For the Experiment 3 coupon, approximately 1 g of AZ-101 evaporated salt was deposited within the glass ring. In Experiment 4, approximately 1 g of AZ-101 evaporated salt mixed with 1 g of Kaolin was deposited within the glass ring. A schematic of the four experimental setups is presented in Figure 4-1. The glass ring was kept in place after making the deposits so the deposits can stay in place for the duration of the test.

| (a) Experiment 1 | (b) Experiment 2 | (c) Experiment 3 and 4 |
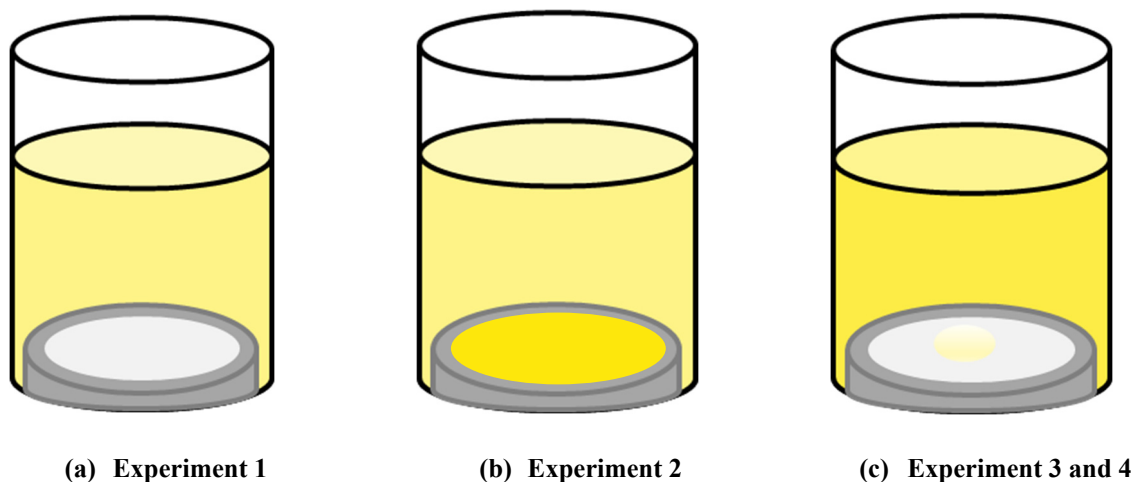
Figure 4-1. Schematic of the underdeposit corrosion tests: (a) Experiment 1, (b) Experiment 2, and (c) Experiments 3 and 4

The coupons along with the simulants were placed in glass beakers. The glass beakers were covered with lids. The beakers were placed in a mineral oil-bath and its temperature was maintained such that the test solutions in each beaker was close to 70 °C. Miscellaneous images of the pre-setup and setup steps are shown in Figure 4-2. An image showing all four experiments in the mineral oil bath is also included in Figure 4-2.
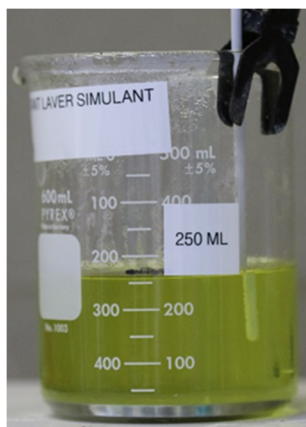
(a) Coupon with AZ-101 simulant for saltcake deposition

(b) AZ-101 evaporate in form of the saltcake at the coupon surface
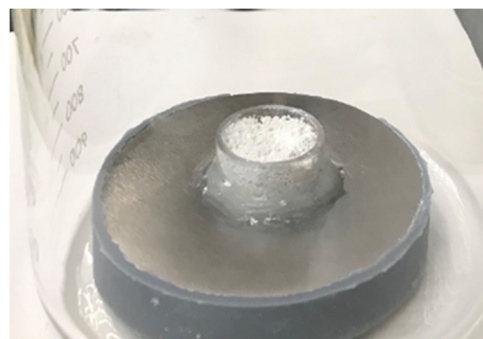
(c) A mounted coupon with glass ring containing kaolin

(d) Coupon with deposits concentrated within the glass ring
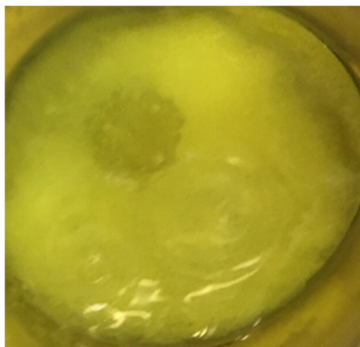
(e) Experiment 1: coupon with no deposits (Control experiment)
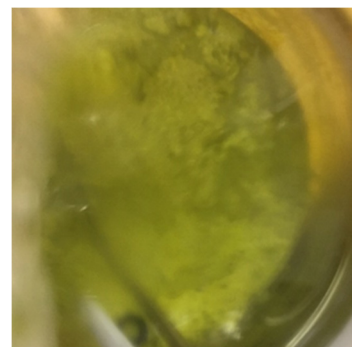
(f) Experiment 2: coupon with deposits covering entire surface
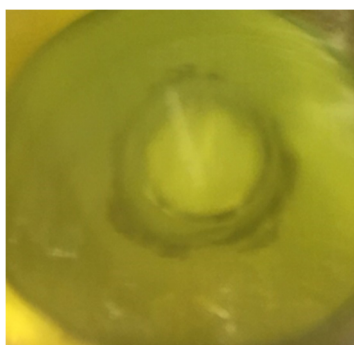
(g) Experiment 3: AZ-101 deposit focused in 1-inch diameter region at the coupon's center
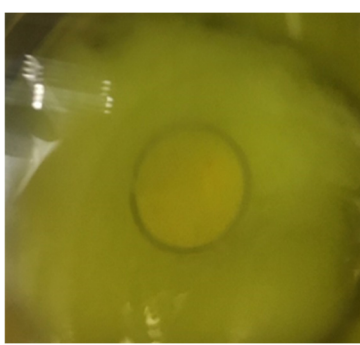
(h) Experiment 4: AZ-101 deposit plus kaolin focused in 1-inch diameter region at the coupon's center
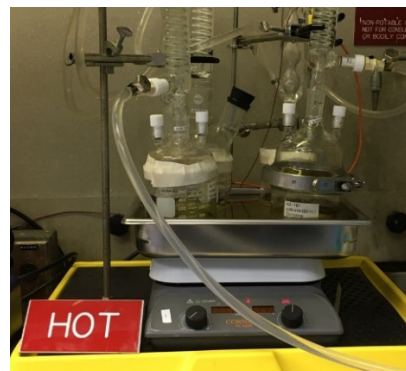
(i) All four experiment setups maintained at 70 °C using the mineral oil bath

Figure 4-2. Images of experimental setup steps of underdeposit/crevice corrosion

4.2 Secondary Liner Corrosion Testing

4.2.1 Materials

Disk coupons, machined from AAR TC 128 steel plate, were used in the secondary liner experiments. The coupons were 25 mm (1 inch) diameter with a thickness of 3 mm (0.125 inch) and polished to a 600-grit finish. The coupons were mounted in a mold prepared with a two-part clear epoxy solution (EpoKwick® from Buehler) so that one face of the coupon was exposed to the test electrolyte. Prior to mounting, each coupon was weighed so that the weight change at the end of the tests could be recorded. An image showing a test coupon is presented in Figure 4-3. The coupons' exposed surface was modified to simulate crevice corrosion. A crevice former was tightly attached to each coupon surface using tape and wire. The crevice formers partially covered the coupons' surfaces, which created conditions for localized corrosion under the crevice formers.
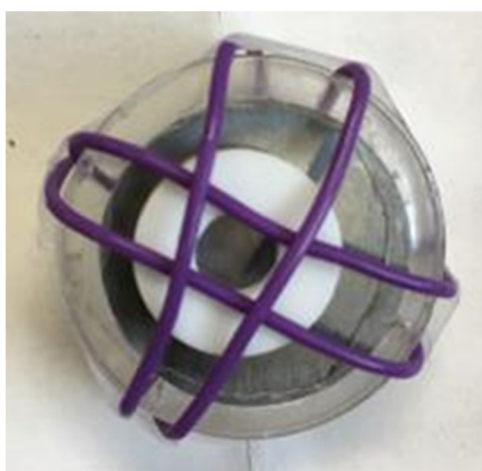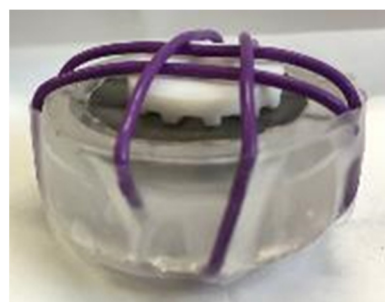
(a) Top view   **(b) Side View**

Figure 4-3. Image of a coupon used in the study. (a) Top, and (b) side views of the partially covered coupon. The coupon's surface was partially covered with a white crevice former, which is held in place using purple wire and tape.

4.2.2 Simulants and VCIs

GW simulant was used for the secondary liner corrosion studies. The composition of the GW simulant is provided in Table 4-4 and is presented in more detail in Appendix A. The pH of the simulant was adjusted using sodium carbonate and acetic acid to 7.6 after preparation. Several VCI formulations were mixed in GW for the study of VCI effects on corroded materials that were recommended by Cortec® using their VCI formulations: VpCI®-337 (liquid), VpCI®-649MF (liquid) and VpCI®-609 (powder). The VCI recommended dosages are labeled as VCI-A and VCI-B and are listed in Table 4-5.

Table 4-4 Composition of GW Simulant

Chemical	Concentration (M)
Sodium bicarbonate	1.750E-03
Calcium hydroxide	1.500E-03
Potassium nitrate	2.400E-04
Strontium Nitrate	2.874E-06
Ferric sulfate	6.250E-04
Sodium Metasilicate, 5-hydrate	6.000E-04
Ferric chloride	7.667E-05
Manganese Chloride	3.100E-04
Acetic Acid	3.000E-04
pH adjusted using sodium carbonate and acetic acid	7.6

Table 4-5 VCI strategy with manufacturer recommended dosage

VCI strategy	VCI product used	Recommended dosage
VCI-A	VpCI-337	10% v/v VpCI-337 in GW simulant (100 mL in VpCI-337 plus 900 mL of GW simulant for 1 L)
VCI-B	VpCI-609 and VpCI-649MF	10% wt. VpCI-609 in GW (100 g VpCI-609 in 1 L of GW) and 0.75% v/v VpCI-649MF in GW (7.5 mL in 1 L of GW)

4.2.3 Testing Apparatus

Glass vessels of dimensions 3.3 ft tall and 5.5-inch diameter were used for each experiment. Approximately 1 to 2 L of simulant was added to a vessel for each experiment. Each vessel had a water jacket around the simulant holding area which was used to circulate warm water to maintain the simulant temperature at 45 ± 2 °C. Each vessel also has several ports, which were used to insert thermocouples and ER probes (only for two vessels). An image showing the three vessels used is presented in Figure 4-4(a). Coupons were exposed to the electrolyte and vapors of the electrolyte in each experiment by suspending them by a rod shown in Figure 4-4(b). The rod holding the coupons was placed inside the vessel. Coupons were suspended from stainless steel rings that are welded to the rod at three different locations. Three vessels were used and for these vessels six coupons were placed at the top, intermediate and low position. Also, six coupons were immersed into the solution. A total of 24 coupons per vessel or 72 coupons overall were utilized. The coupons' positions, with respect to electrolyte in each vessel, simulated different vapor space conditions and water levels in the drain slots. These levels are described as follows.

Level 1: Bottom or low level. Coupons were dipped in the simulant for five minutes prior to testing. The coupons were hung at the bottom fixed ring of the rod shown in Figure 4-4(b). These coupons were suspended approximately 1 inch above the liquid level of the simulant. Every two weeks, the coupons were lowered into the simulant for 5 minutes. This level is representative of the situation when secondary liner bottom plate experienced periodic wetting/drying.

Level 2: Intermediate or middle level. Coupons were dipped in the simulant for five minutes prior to testing. The coupons were hung at the middle-fixed ring approximately 18 inches above the liquid simulant in each vessel. This level is representative of a vapor space region of the secondary liner bottom that at one time was exposed to water but has had infrequent or no contact with the water since that time. However, this region is exposed to the humidified air.

Level 3: Top or high level. This set of coupons was not exposed to the solution prior to testing. The coupons were suspended approximately 36 inches above the simulant. This level is representative of the secondary liner bottom plate region that is only exposed to the humidified air and any volatile species from the solution.

(a) **(b)**

Figure 4-4 Images of the (a) experimental configuration, and (b) steel rod to suspend the coupons inside the vessel containing electrolyte.

Table 4-6 lists the vessel and the corresponding VCI strategy used. Vessels 1 and 2 had 100% of the recommended dosage of VCI-A and VCI-B, respectively. Vessel 3 had 50% of the recommended dosage of VCI-B. ER probes were placed in Vessels 1 and 2, near the coupons at Level 1. ER probe data was collected periodically. Six coupons from each position were removed after two months. Then, the corresponding VCI solution (VCI-A or VCI-B) was added and the rest of the coupons were exposed for an additional four months. Coupons that were removed were cleaned with Clarke's solution [11] to remove corrosion products. The coupons were then weighed and the difference between the final and initial weight was recorded.

Table 4-6 Experimental details of Vapor Space Corrosion Setup

Vessel	VCI strategy
1	GW + 100% of recommended dosage VCI-A
2	GW + 100% of recommended dosage VCI-B
3	GW + 50% of recommended dosage VCI-B

4.3 Open Circuit Potential Drift Testing

4.3.1 Sample preparation

The electrochemical testing including long-term OCP measurements were performed by using electrodes in a "bullet" shape with dimensions: 0.188 inch in diameter and 1.25 inches long (Metal Samples Company part number EL-400). In Figure 4-5, an image of the sample after being polished and rinsed is shown. Before testing, a drill was used to rotate the sample and grind it to a uniform 600 grit finish. Afterwards, the sample was rinsed with distilled water and then acetone. The bullets were visually examined for any defects and to ensure that the sample had a uniform surface preparation. The sample was then attached to a stainless steel rod protected by a glass holder. A polytetrafluoroethylene (PTFE) fixture was used to prevent liquid contact with the stainless-steel rod and ensure electrical isolation.
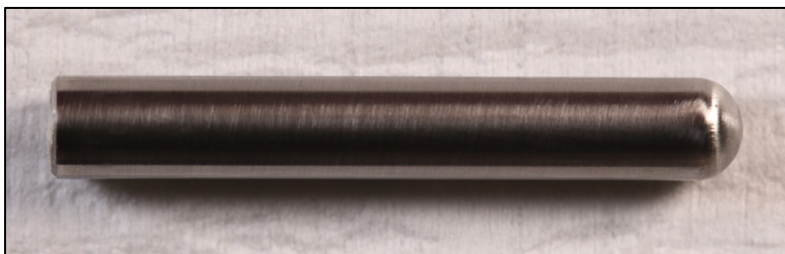
Figure 4-5. Side view image of the "bullet" shaped coupon

Long-term potential drift testing also involved using coupons with mill-scale and corrosion products. These coupons were fabricated by cutting 1.5 cm × 1.5 cm of AAR TC-128 metal plate with mill-scale plus corrosion products. The plate was cut using an Electrical Discharge Machine (EDM). The samples were connected to a wire for electrical connection using silver epoxy, then mounted with a two-part clear epoxy solution (EpoKwick from Buehler) so that one face of the coupon was exposed. Figure 4-6 shows an image of the mill-scale coupons used in the testing.
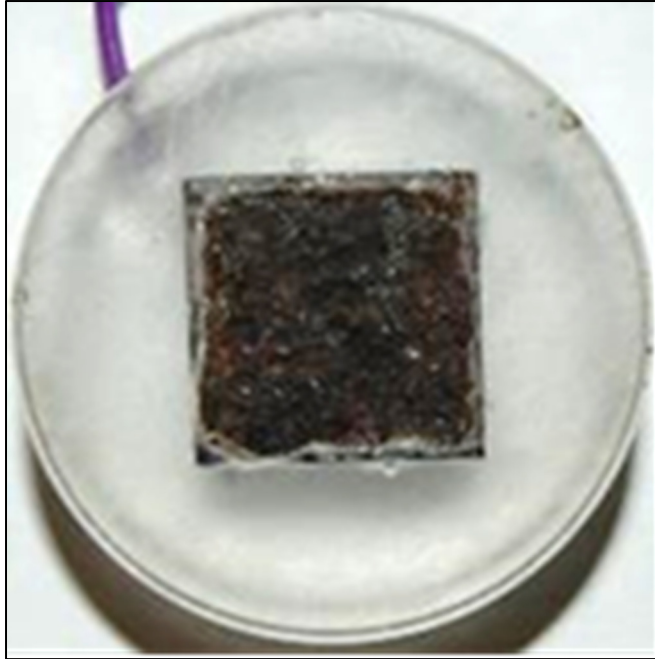
Figure 4-6. Image of a coupon with mill-scale used to study evolution of OCP

Long-term potential drift testing also involved using coupons with surfaces only partially covered with mill-scale plus corrosion products: these coupons were modified versions of the coupons with mill-scale plus corrosion products surfaces. After fabricating the mill-scale plus corrosion product coupons, approximately one fourth of the coupons' surfaces were machined to remove the mill-scale and corrosion product layers. An image of such coupon is presented in Figure 4-7; these are identified as partial mill-scale coupons.
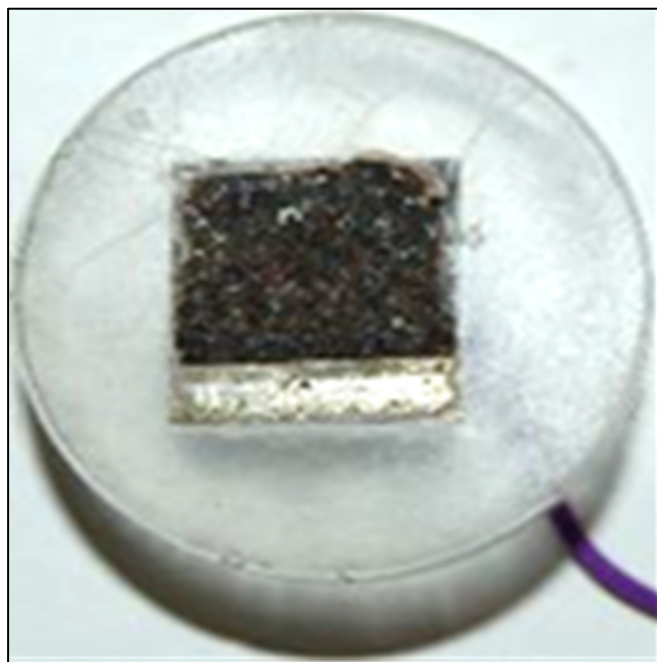
Figure 4-7. Image of a partial mill-scale coupon used to study evolution of OCP

4.3.2 Simulants

Three Hanford waste simulants were used as the electrolytes to study the OCP evolution. These simulants are identified as AY-101, AW-105, and SY-101. To study the effects of organics species in AW-105, three variants of the AW-105 simulant were prepared: (i) AW-105 with small-chain organic acids, such as formate, acetate, and glycolate, which will be referred to as AW-105 Base, (ii) AW-105 with small-chain organic acids, the TBP family organics, and the NPH, which will be referred to as AW-105 Representative and (iii) AW-105 with small-chain organic acids, spiked TBP family organics, and NPH, which will be referred to as AW-105 Elevated TOC. The chemical composition of the AY-101, AW-105 with small-chain organics (i.e., AW-105 Base), and SY-101 are listed in Table 4-7. The chemical compositions of the AW-105 with small-chain organic acids plus TBP and NPH organics (i.e., AW-105 Representative and AW-105 Elevated TOC) are partially listed in Table 4-8; the remaining species in this simulant are same as in AW-105 Base. Note that AW-105 Representative aligns with the sample analysis from the tank.

Table 4-7. Chemical composition of the simulants used to study evolution of OCP

| Chemical	Concentration (M)		
	AY-101	**AW-105 Base**	**SY-101**
Sodium hydroxide	0.688	1.735	0.600
Sodium nitrite	1.251	1.000	0.259
Sodium nitrate	1.911	1.101	1.032
Sodium chloride	0.070	0.046	0.027
Sodium fluoride	0.025	0.108	0.021
Sodium sulfate	0.056	0.021	0.020
Trisodium phosphate, 12-hydrate	0.036	0.012	0.083
Sodium carbonate	0.743	0.751	0.206
Sodium bicarbonate	0.000		0.001
Sodium formate	0.026	0.008	0.010
Sodium acetate, 3-hydrate	0.012	0.012	0.003
Sodium glycolate	0.0029		0.003
Sodium oxalate	0.0062	0.004	0.022
Ammonium bicarbonate	0.0013	0.00866	0.006
Sodium aluminate	0.261	0.324	0.131
Potassium nitrate	0.089	0.719	0.008
Solution pH at 21 °C	14	14	14

Table 4-8. Chemical composition of AW 105 simulants with additional TOC

Chemical	Concentration (M)	
	AW-105 Representative	**AW-105 Elevated TOC**
Propionic acid	0.0000703	0.0000703
Sodium acetate, 3 hydrate	0.012	0.12
Sodium glycolate	0.0029	0.029
Sodium butyrate	0.000149	0.000149
Tributyl phosphate	0.0000412	0.0000412
1-Butanol	0.000177	0.000177
n-butyl phosphate: mixture of mono-n-butyl and di-n-butyl	0.0034	0.034
Bis(2-ethylhexyl)phthalate	2.80E-06	2.80E-06
2-methyl-2-nitrobutane (tert-nitrobutane)	0.000719	0.000719
tetradecanoate (myristic acid)	1.00E-05	1.00E-05
Butanone-2 (ethyl methyl ketone)	0.00001	0.00001
Methylbutanone-2 (3-hydroxy-3-methyl-2-butanone)	0.00001	0.00001
Undecane	1.00E-08	1.00E-08
Dodecane	1.00E-08	1.00E-08
Tridecane	1.00E-08	1.00E-08
Tetradecane	1.00E-08	1.00E-08
1-Octanol	1.00E-06	1.00E-06
2-Octanone	1.00E-06	1.00E-06
Octanoate (ethyl octanoate)	1.00E-05	1.00E-05
1-Tetradecanol (myristyl alcohol)	1.00E-06	1.00E-06
2-Tetradecanone	1.00E-06	1.00E-06

All experiments were conducted at 35 °C, and atmospheric pressure. All potentials were measured with respect to Saturated Calomel Electrode (SCE) references.

4.3.3 Testing Apparatus

A glass corrosion cell with approximately 700 mL of simulant was used for electrochemical testing and long-term OCP drift. A picture of the setup is shown in Figure 4-8. A carbon rod was used as the counter electrode for the LPR, CPP and EIS measurements. A SCE was used as the reference electrode and placed in a salt bridge with a glass frit. The bridge solution was 0.1 M $NaNO_3$. Prior to each test, the electrode was checked against a standard (a SCE in 1 M KCl solution that was not used for testing) and several times during long-term testing. The cell was placed on top of a hotplate and the temperature was maintained by

a thermocouple from the hotplate immersed in solution. REF600 and Interface E (Gamry) potentiostats were used in this study. Prior to initiating the electrochemical tests, ASTM G5 [12] was performed for quality assurance. ASTM G5 protocols were also run at the conclusion of testing. The standardized CPP protocol was used to gather the data [13]. In several instances, EIS scans were performed over a wide frequency range. At the end of testing, the standard CPP protocol was used to test the susceptibility to localized corrosion.

For long-term OCP drift testing, a multiplexer (Gamry) was used to obtain OCP values for each of the six coupons. Three corrosion cells were used, each with three working electrodes. OCP was measured every 10 seconds within the first week (i.e., 1-2 days) of starting the experiment and then every hour for approximately 4 months.
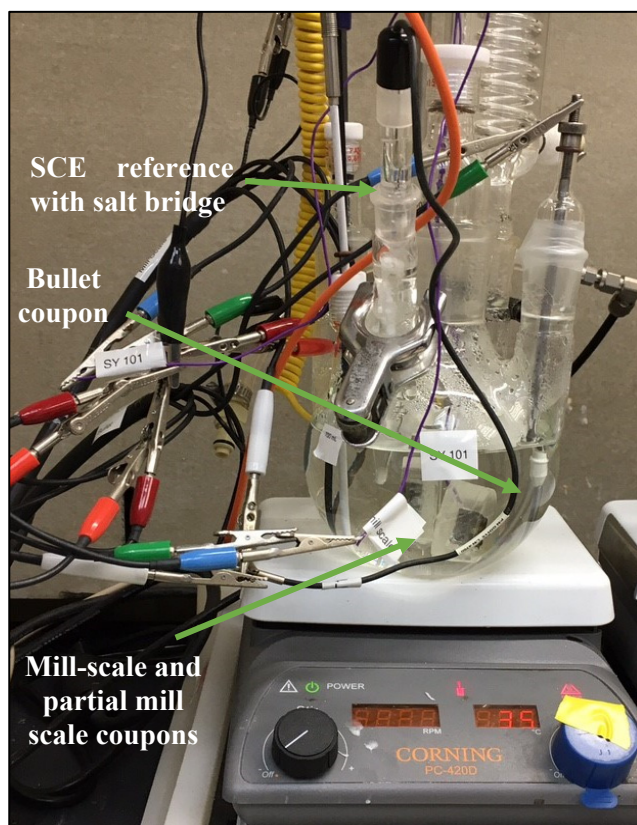
Figure 4-8. Image of the experimental setup used for the OCP drift experiments.

4.4 Quality Assurance

Data for all Tasks were recorded in the electronic laboratory notebook system, notebook number G8519-00126.

Requirements for performing reviews of technical reports and the extent of review are established in manual E7 2.60. SRNL documents the extent and type of review using the SRNL Technical Report Design Checklist contained in WSRC-IM-2002-00011, Rev. 2.

5.0 Results and Discussion

The results and discussion for the report are enumerated by the corresponding task.

5.1 New Limits Corrosion Testing

A test that was part of the FY17 report [5] that consisted of a dilute chemistry and no nitrite concentration was investigated. This test corresponded to Test 6 of the High Hydroxide Matrix, which is shown in Table 4-2 of the FY17 report [5]. As listed in Table 5-1, based on the chemical composition, the PF is 1.95, which would qualify this test as a pass since it is above the limit established of 1.2 [1]. However, after performing CPP testing, a category 3 result was obtained for this condition in the duplicate runs as shown in Figure 5-1. The sample and duplicate followed similar CPP scans. The forward scans continued until trans-passive potentials and the reverse scans abruptly went to higher currents while the potentials were scanned in the negative direction. Based on the CPP tests and pitting occurrence in the sample, as seen at the left side of the CPP scans, the tests were considered fails.

Table 5-1. Test 6 from High hydroxide statistically selected simulant chemistries matrix

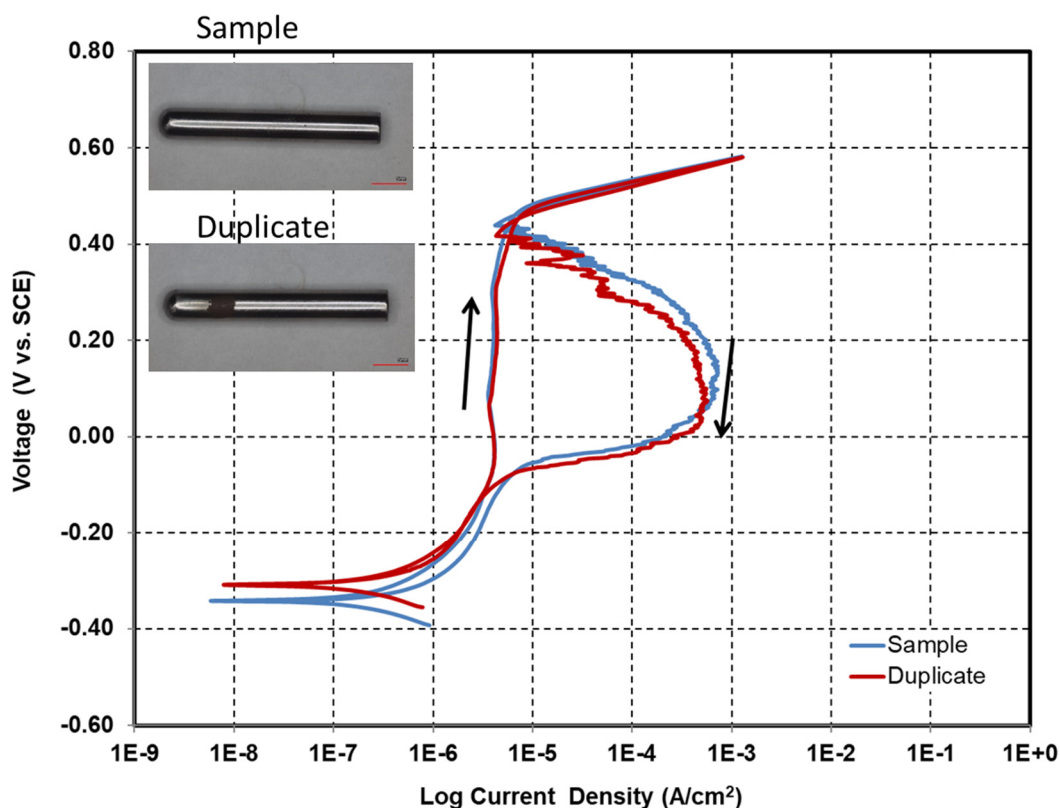| Test	Temperature (°C)	Hydroxide (M)	Nitrite (M)	Nitrate (M)	Chloride (M)	Sulfate (M)	Carbonate (M)	PF
6	35	1.2	0	0.94	0.24	0.01	0.1	1.95

Figure 5-1. CPP results of Test 6 from High Hydroxide statistically selected chemistries matrix and, pictures of sample and duplicate bullet coupon after test [5]]

The coupons images in Figure 5-1 exhibited small pits on the shank and with a larger cluster of pits on the nose, with the duplicate displaying a large cluster of pits on the shank. The location of the pits and corroded area did not affect the CPP results, as they are similar. A recommendation was made by the TIEP corrosion sub-group to perform a potentiodynamic-potentiostatic test. The potential was scanned from the OCP in the positive direction until it reached 200 mV$_{SCE}$. The potentiostatic test was conducted at this potential for several hours to allow for pit initiation and growth. Figure 5-2 presents the CPP result for this test. The potentiodynamic test in Figure 5-2 (a) is similar to the CPP forward scan in Figure 5-1 up to 200 mV$_{SCE}$. Then, while holding the potential at 200 mV$_{SCE}$, a dramatic increase was observed after 25 hours with the current density reaching a maximum of 1.43 mA/cm^2 as seen in Figure 5-2 (b). A decrease to approximately 0.8 mA/cm^2 occurred after and the current remained around this value for 10 hours. Following this 10-hour period of increased current density, the current density remained low, but fluctuated slightly between 20-80 uA/cm^2.
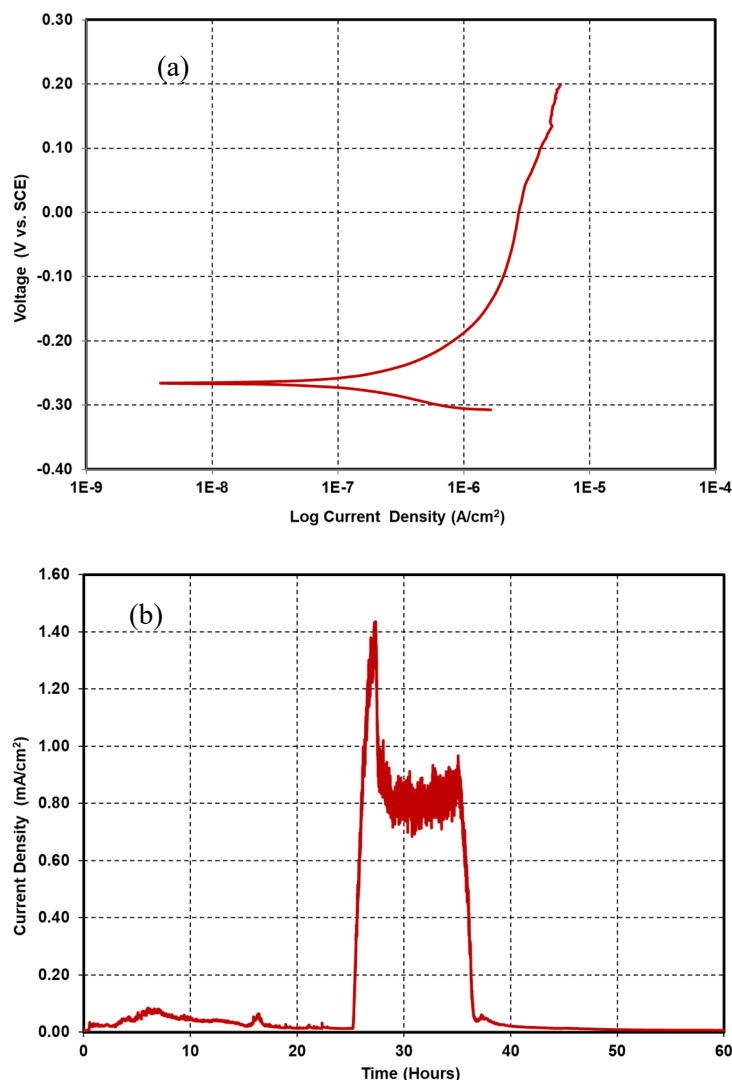
Figure 5-2. (A) Potentiodynamic, and (B) Potentiostatic hold for 60 hours of Test 6 from the high hydroxide statistically selected chemistries matrix

Images of the sample after the test are shown in Figure 5-3. The sample corroded uniformly with shallow pits observed in the Laser Confocal Microscope (LCM) images (C and D). It appears that there are tiny pits (~60 µm in diameter) uniformly distributed on the surface with a maximum depth of ~40 µm. The height profile with color gradation shows the relative pit depths, with blue being the deepest and yellow approximating the surface.

Figure 5-3. Images of nose (A) and shank (B) of bullet coupon. LCM image (C) and height profile of coupon (D).

A CPP test was performed in the same solution, except that a small amount of nitrite was added (i.e., 0.2 M). Figure 5-4 shows the CPP result indicating category 1 or negative hysteresis. Thus, the presence of 0.2 M nitrite was sufficient to mitigate the pitting attack. The obtained result, in conjunction with other tests in the matrix, was used to help establish the limits for minimum nitrite concentration to be 0.2 M.
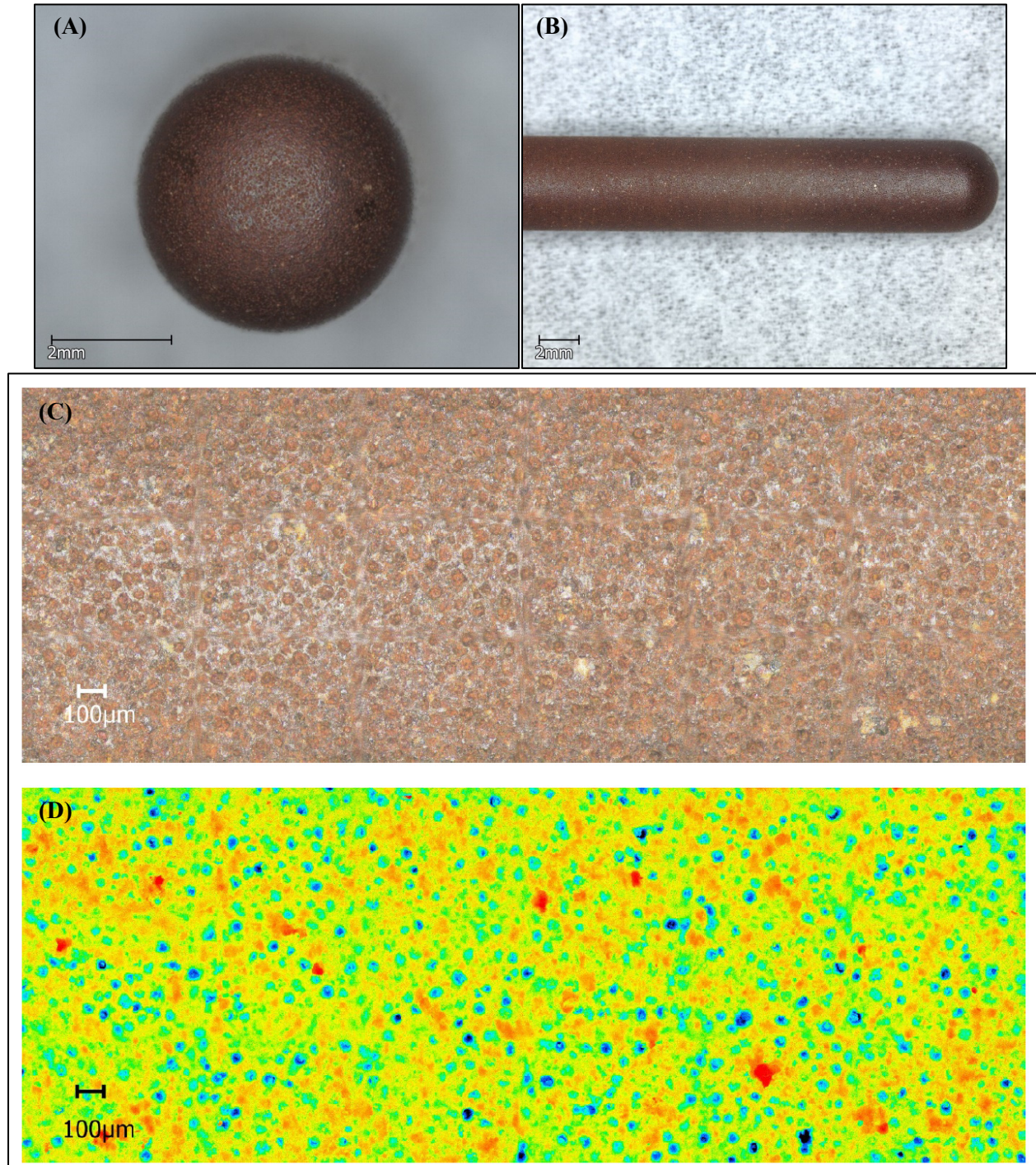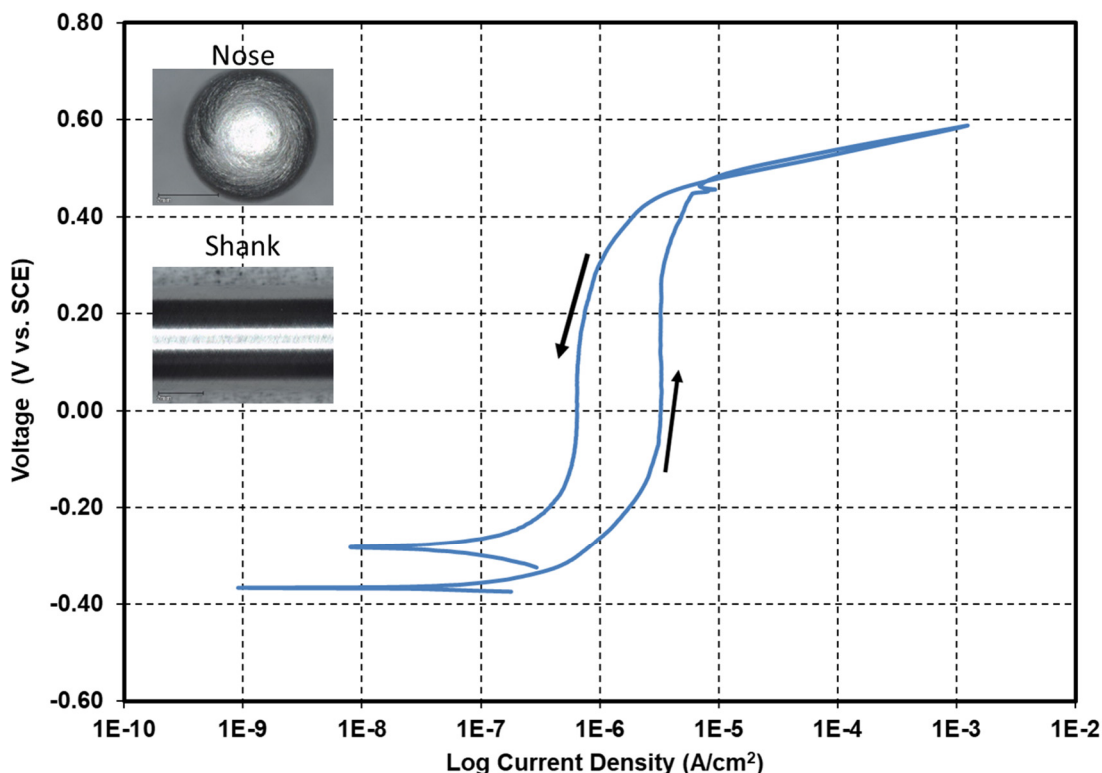

Figure 5-4. CPP results of Test 6 from High Hydroxide statistically selected chemistries matrix with 0.2 M addition of nitrite and, pictures of nose and shank of the bullet coupon after test.

5.2 Underdeposit Corrosion Testing

The overall approach involved using Tank AZ-101 interstitial liquid simulant to assess the risk of corrosion of the tank steel, with and without the presence of deposited solids. The PF for AZ-101 interstitial liquid is approximately 4, therefore, its pH will be adjusted to lower the pitting factor within the 1-2 range, which may increase pitting susceptibility in the crevice. Four tests were conducted as per the details listed in Table 4-3 .

5.2.1 OLI Simulations of Modified AZ-101

Solubility of the AZ-101 evaporated saltcake in the AZ-101 simulant was explored using the software OLI Studio: Stream Analyzer from OLI systems, Inc. where input and output species of a modified AZ-101 simulant were initially verified. If the input and output species are the same, it implies that the input composition is stable at standard temperature and pressure. Input composition of the AZ-101 was slightly modified by replacing the propionic acid with sodium acetate. Inputs and output species of the simulant are listed in Table 5-2. The input and output streams' concentrations are identical, indicating that the input

stream is thermodynamically stable, and would not result in precipitation at the standard temperature and pressure.

Table 5-2. OLI stream input and output concentrations

Species	Input Stream (mol/L)	Output Stream (mol/L)
H_2O	48.4008	48.4008
KNO_3	0.12	0.12
$NaNO_2$	1.6	1.6
$NaNO_3$	0.826	0.826
Na_2SO_4	0.05	0.05
Na_2CO_3	0.57	0.57
$Na[C_2H_3O_2].3H_2O$	7.50E-04	7.50E-04
NaF	0.102	0.102
$NaOH$	0.081	0.081
$Na_3PO_4.8H_2O$	0.02	0.02
$Na_2CrO_4.4H_2O$	1.00E-03	1.00E-03
$B(OH)_3$	1.00E-03	1.00E-03

A liquid simulant with the output stream composition in Table 5-2 was heated at 120 °C and 1 atm until the liquid had evaporated.. The precipitated solids, or boil-off, were mixed with the modified simulants at 70 °C. The resulting output is listed in Table 5-3.

Table 5-3. OLI analysis of AZ-101 boil-off mixed with the simulant

Species	Total Amount (mol)	Aqueous Phase (mol)	Solid Phase (mol)
H_2O	48.5733	48.5733	
Na^{+1}	3.78685	3.78685	
NO_2^{-1}	1.6003	1.6003	
NO_3^{-1}	0.797046	0.797046	
CO_3^{-2}	0.473289	0.473289	
$NaSO_4^{-1}$	0.157212	0.157212	
$NaNO_3$ (Nitratine)	0.149133	0.149133	0
F^{-1}	0.14555	0.14555	
K^{+1}	0.111992	0.111992	
$NaCO_3^{-1}$	0.095822	0.095822	
OH^{-1}	0.082898	0.082898	
$NaF \cdot Na_2SO_4$ (Kogarkoite)	0.077328		0.077328
NaF (Villiaumite)	0.067594	0.067594	0
PO_4^{-3}	0.01812	0.01812	
Na_2F^{+1}	0.011548	0.011548	
KSO_4^{-1}	8.02E-03	8.02E-03	
SO_4^{-2}	7.45E-03	7.45E-03	
HPO_4^{-2}	1.88E-03	1.88E-03	
CrO_4^{-2}	1.00E-03	1.00E-03	

Table 5-3. OLI analysis of AZ-101 boil-off mixed with the simulant

Species	Total Amount (mol)	Aqueous Phase (mol)	Solid Phase (mol)
HCO_3^{-1}	8.78E-04	8.78E-04	
$B(OH)_4^{-1}$	6.40E-04	6.40E-04	
$C_2H_3O_2^{-1}$	4.21E-04	4.21E-04	
$NaB(OH)_4$	3.60E-04	3.60E-04	
$Na[C_2H_3O_2]$	3.22E-04	3.22E-04	0
$NaHCO_3$ (Nahcolite)	1.19E-04	1.19E-04	0
$K[C_2H_3O_2]$	7.70E-06	7.70E-06	
$B(OH)_3$	4.06E-07	4.06E-07	0
$P_2O_7^{-4}$	1.89E-08	1.89E-08	
$BF(OH)_3^{-1}$	1.37E-08	1.37E-08	
$H_2PO_4^{-1}$	2.52E-09	2.52E-09	
$B_2O(OH)_5^{-1}$	2.00E-09	2.00E-09	
$HCrO_4^{-1}$	6.24E-10	6.24E-10	
CO_2	5.53E-10	5.53E-10	
HNO_2	5.11E-10	5.11E-10	
HF	1.84E-10	1.84E-10	
CH_3COOH	2.07E-11	2.07E-11	
HF_2^{-1}	1.92E-11	1.92E-11	
HSO_4^{-1}	4.87E-12	4.87E-12	
H^{+1}	1.57E-12	1.57E-12	
$HP_2O_7^{-3}$	4.29E-13	4.29E-13	
$BF_2(OH)_2^{-1}$	1.25E-13	1.25E-13	
$B_3O_3(OH)_4^{-1}$	4.78E-14	4.78E-14	
$KHSO_4$ (Mercallite)	4.47E-15	4.47E-15	0
$B_4O_5(OH)_4^{-2}$	7.09E-16	7.09E-16	
HNO_3	7.90E-17	7.90E-17	
$Cr_2O_7^{-2}$	7.10E-17	7.10E-17	
$H_2P_2O_7^{-2}$	6.57E-19	6.57E-19	
H_3PO_4	2.06E-19	2.06E-19	
BF_3OH^{-1}	2.01E-21	2.01E-21	
$(HF)_2$	1.01E-23	1.01E-23	
BF_4^{-1}	2.79E-28	2.79E-28	
$C_4H_8O_4$	5.03E-29	5.03E-29	
$H_3P_2O_7^{-1}$	1.36E-29	1.36E-29	
H_2SO_4	1.08E-34	1.08E-34	
SO_3	3.40E-38	3.40E-38	
$H_4P_2O_7$	5.41E-40	5.41E-40	
HBF_4	3.30E-43	3.30E-43	

Table 5-3. OLI analysis of AZ-101 boil-off mixed with the simulant

Species	Total Amount (mol)	Aqueous Phase (mol)	Solid Phase (mol)
Total (by phase)	56.1691	56.0918	0.077328

OLI simulation indicated that evaporation of the AZ-101 simulant will result in formation of salt complex $NaF \cdot Na_2SO_4$ (Kogarkoite) saltcake that will not re-dissolve back in the AZ-101 simulant.

A CPP test for a bullet coupon in AZ-101 simulant is presented in Figure 5-5. As seen in the figure, the data indicate that the pitting corrosion of the coupons without deposits is not likely.
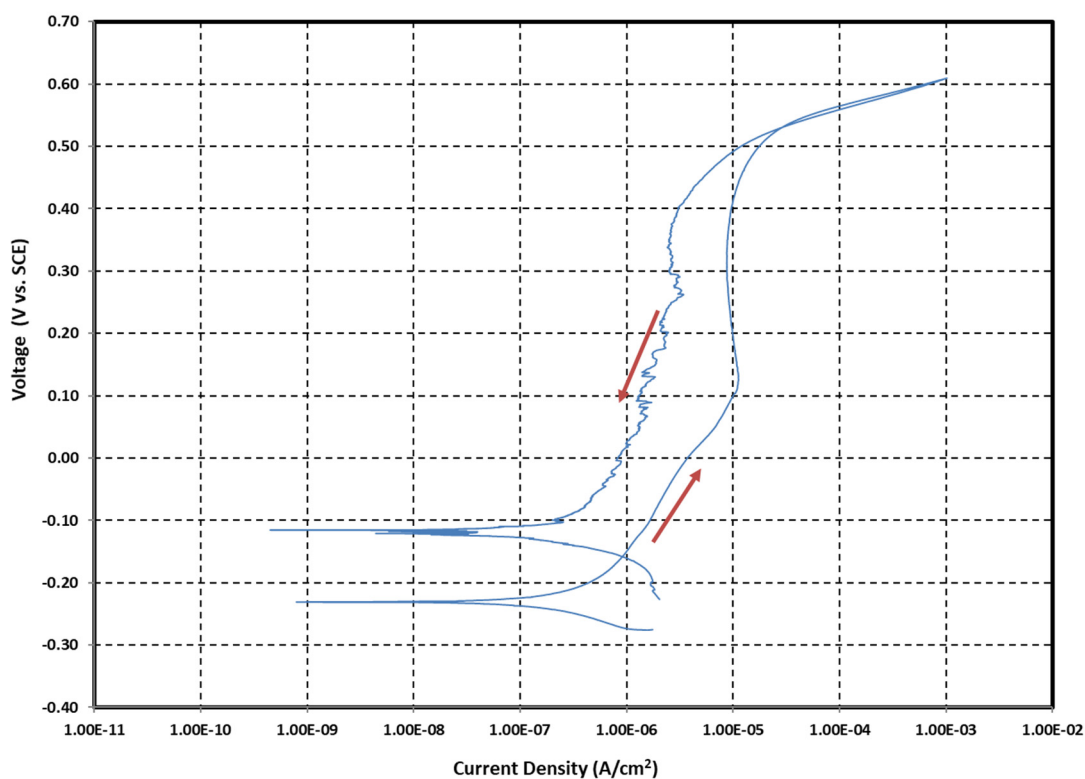

Figure 5-5. CPP curve of a bullet coupon in AZ-101 Simulant without deposits

The coupon mass data from the four experiments after four months of exposure is listed in Table 5-4. The Experiment 1 coupon mass loss was 0.2 mg, which corresponded to the corrosion rate of 0.4 µm/yr (0.016 mpy). This low corrosion rate indicated that corrosion of the coupon was negligible. The Experiment 2 coupon lost 1 mg, which translated into corrosion rate of 2 µm/yr (0.08 mpy). This is still a very-low corrosion rate and is not indicative of significant underdeposit corrosion. The Experiment 3 coupon lost 5 mg; a closer examination of the coupon surface indicated that the corrosion occurred directly underneath the glass ring and silicone material, and no corrosion was observed below the saltcake deposits. The Experiment 4 coupon gained 9 mg; indicating absence of corrosion under the saltcake plus kaolin deposits.

Profiled images of the coupons before and after exposure are presented in Table 5-5. There is no sign of pitting corrosion on any of the Experiments 2, 3, and 4 coupons, indicating that underdeposit corrosion did

23

not occur in any of the three coupons. The lack of noticeable corrosion was likely due to the loose nature of the salt deposits, which allowed for relatively easy access for the inhibited interstitial simulant to diffuse to the surface of the coupon. Further testing on coupons with an adherent solid deposit that limits the diffusion and potentially creates a crevice or partially covered area is warranted. In FY21, an AZ-101 sludge solid simulant will be prepared to create a representative adherent solid in an attempt to create a realistic underdeposit.

Table 5-4. Underdeposit corrosion study coupon mass data and corrosion rates

Experiment Identification	Initial Mass (g)	After Exposure Mass (g)	Corrosion Rate (µm/yr)
Experiment 1 (Control experiment)	121.6152	121.6150	0.4
Experiment 2 (AZ-101 evaporate deposits distributed throughout coupon surface)	121.9040	121.9030	2.0
Experiment 3 (AZ-101 evaporated salt deposits focused on the 1-inch disk at the coupon's center)	121.2324	121.2274	9.8
Experiment 4 (AZ-101 evaporated salt deposits plus kaolin deposits focused on the 1-inch disk at the coupon's center)	121.8819	121.8909	NA

Table 5-5. Profiled images of the underdeposit corrosion coupons before and after exposure
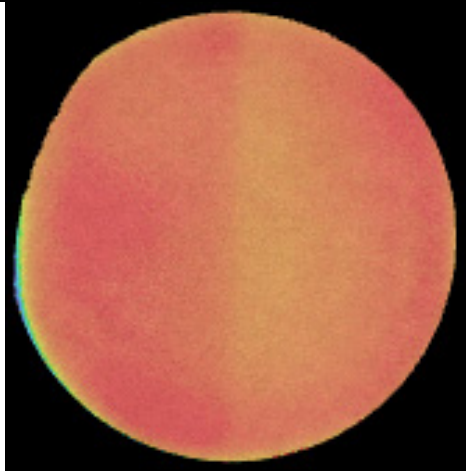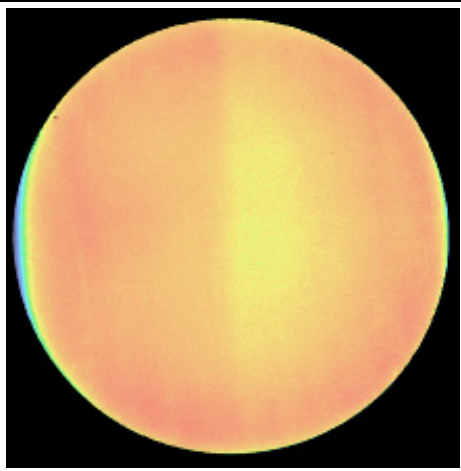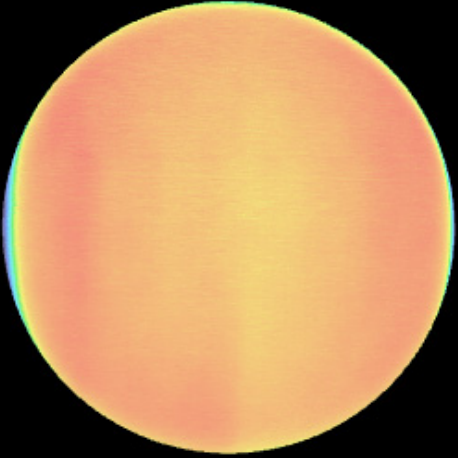
Experiment Identification	Before Exposure	After Exposure
Experiment 1 (Coupon 1)		

Table 5-5. Profiled images of the underdeposit corrosion coupons before and after exposure

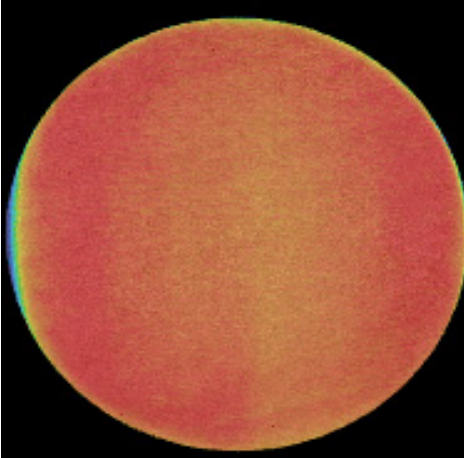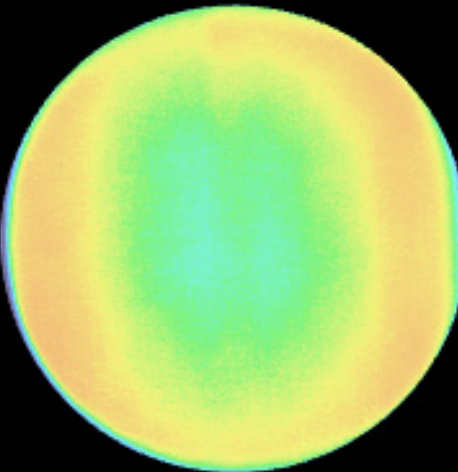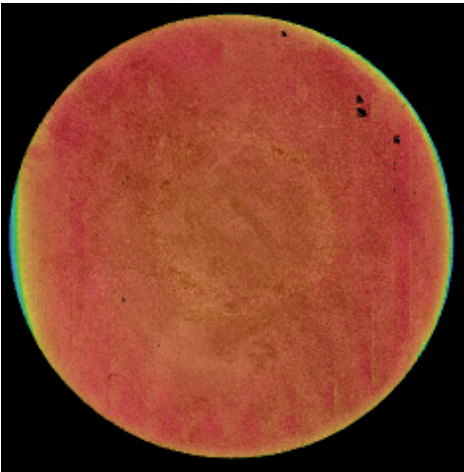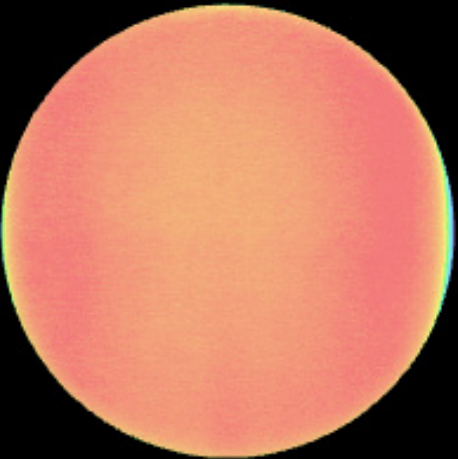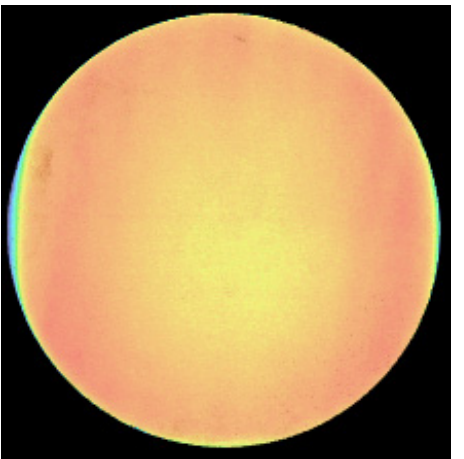| Experiment Identification	Before Exposure	After Exposure
Experiment 2 (Coupon 2)		
Experiment 3 (Coupon 3)		
Experiment 4 (Coupon 4)		

5.4 Secondary Liner Corrosion

The pictures of the samples after exposure and cleaning for this task are shown in Appendix B. Vessel identification, coupon and ER probe location information is summarized in Table 5-6. The corrosion rate data for the coupons treated with 100% of recommended dosages of VCI-A in Vessel 1 and VCI-B in Vessel 2 are listed in Table 5-7 and Table 5-8, respectively. Similarly, the corrosion rate data for the coupons treated with 50% of the recommended dosage of VCI-B are listed in Table 5-9. The corrosion rate data obtained for each coupon were: (i) surface average corrosion rate, and (ii) maximum pitting corrosion rate. The surface average corrosion rate for each coupon was obtained by recording mass loss and exposure time. The maximum pitting corrosion rate was obtained by measuring the deepest pit on each coupon. Table 5-7 has surface average and pitting corrosion rate data for the GW (2-month) and then GW plus 100% recommended dosage of VCI-A (6-month), and Table 5-8 has the data for the GW (2-month) and then GW plus 100% recommended dosage of VCI-B (6-month). Similarly, Table 5-9 has the data for the GW (2-month) and then GW plus 50% recommended dosage of VCI-B (6-month). The 2-month coupons were exposed to GW simulant, whereas 6-month coupons were exposed to GW only for the first two months and then to GW plus VCI dosages for an additional four months. The tables' data also include average of surface average and pitting corrosion rates along with corresponding standard deviations. These average values and standard deviations are presented in Figure 5-6 (from Table 5-7 data) and Figure 5-7 (from Table 5-8 data) and Figure 5-8 (from Table 5-9 data).

Table 5-6. Vessel identification Solution, and coupons and ER probe information

Vessel	Solution	Notes
1	Initially GW simulant, and then 100% of the recommended dosage of VCI-A after 2 months	• 6 coupons each in immersed, Level 1, Level 2, and Level 3 positions, total 24 coupons. • ER probes at each level. Cylindrical element probes at immersed, Levels 1 and 2, and wire element probe at Level 3.
2	Initially GW simulant, and then 100% of the recommended dosage of VCI-B after 2 months	• 6 coupons each in immersed, Level 1, Level 2, and Level 3 positions, total 24 coupons. • ER probes at each level. Cylindrical element probes at immersed, Levels 1 and 2, and wire element probe at Level 3.
3	Initially GW simulant, and then 50% of the recommended dosage of VCI-B after 2 months	• 6 coupons each in immersed, Level 1, Level 2, and Level 3 positions, total 24 coupons. • Cylindrical element probe at Level 2 and wire element probe at Level 3.

Table 5-7. Vessel 1 (100% VCI-A After Two Months) Coupon Corrosion Data

Corrosion Type	Corrosion Rate (µm/yr)*							
	Immersed		Level 1		Level 2		Level 3	
	2-month	6-month	2-month	6-month	2-month	6-month	2-month	6-Month
Surface Average Corrosion	145	61	58	41	91	43	74	41
	165	61	56	36	74	30	74	41
	137	61	145	58	48	36	33	25
Average ± std***	149 ± 14.4	61 ± 0	86.4 ± 50.6	44.9 ± 12	71.1 ± 21.7	36.4 ± 6.4	60.1 ± 23.5	35.6 ± 8.8
Pitting Corrosion	457	127	965	279	1168	356	1092	305
	457	152	787	229	1041	432	762	381
	508	305	1016	279	635	203	533	254
Average ± std***	474 ±29	195 ± 96	923 ± 120	263 ± 29	948 ± 279	330 ± 116	796 ± 281	313 ± 64

*25 µm/yr = 1 mil/yr = 1 mpy
**Average values are calculated for 3 coupons
***std denotes standard deviation of the corrosion rate data used to calculate the average

Table 5-8. Vessel 2 (100% VCI-B After Two Months) Coupon Corrosion Data

Corrosion Type	Corrosion Rate (µm/yr)*							
	Immersed		Level 1		Level 2		Level 3	
	2-month	6-month	2-month	6-month	2-month	6-month	2-month	6-Month
Surface Average Corrosion	114	84	79	51	112	41	33	38
	130	76	102	36	76	51	64	36
	130	86	102	38	102	56	81	36
Average ± std***	125 ± 9	82 ± 5	94 ± 13	42 ± 8	97 ± 18	49 ± 8	59 ± 24	36 ± 2
Pitting Corrosion	432	178	864	330	787	254	686	483
	533	152	813	305	711	406	1092	229
	457	152	813	203	533	381	1118	279
Average ± std***	474 ±53	161 ±15	830 ± 29	279 ± 67	677 ± 130	347 ± 82	965 ± 242	330 ± 134

*25 µm/yr = 1 mil/yr = 1 mpy
**Average values are calculated for 3 coupons
***std denotes standard deviation of the corrosion rate data used to calculate the average

Table 5-9. Vessel 3 (50% VCI-B After Two Months) Coupon Corrosion Data

| Corrosion Type	Corrosion Rate (µm/yr)*							
	Immersed		Level 1		Level 2		Level 3	
	2-month	6-month	2-month	6-month	2-month	6-month	2-month	6-Month
Surface Average Corrosion	99	51	58	25	66	18	48	8
	122	56	74	18	64	66	25	53
	127	46	43	23	51	58	33	79
Average** **± std*****	116 ± 15	51 ± 5	58 ± 15	22 ± 4	60 ± 8	47 ± 26	36 ± 12	47 ± 36
Pitting Corrosion	914	305	1168	305	1092	229	1143	254
	1245	686	914	305	584	203	1092	254
	1118	635	813	381	610	203	483	305
Average** **± std*****	1092 ± 167	542 ± 207	965 ± 183	330 ± 44	762 ± 286	212 ± 15	906 ± 368	271 ± 29
*25 µm/yr = 1 mil/yr = 1 mpy **Average values are calculated for 3 coupons ***std denotes standard deviation of the corrosion rate data used to calculate the average								

Vessel 1 corrosion rate data in Figure 5-6 show that 100% VCI-A dosage decreased the corrosion rates at all levels. In Figure 5-6, the 6-month immersed coupons' surface average and pitting corrosion rates are lower than the 2-month coupons' corrosion rates. This result indicates that addition of VCI-A helps arrest propagation of corrosion, both extent of corrosion and pitting depths.

Similarly, Vessel 2 corrosion rate data in Figure 5-7 show that 100% VCI-B dosage decreased the surface average and pitting corrosion rate of the coupons at all levels as well. In most cases for Vessel 3, the data in Figure 5-8 show that the surface average and pitting corrosion rates are decreased due to addition 50% of the recommended dosage of VCI-B. However, at Level 3, the surface average corrosion rate for 6 months is greater than that for the 2 month data. Significant variability in the 6-month coupon data is the cause of this observation, however, the reason for the variability is not known.

A statistical analysis was conducted to determine significance of the decrease in corrosion rate due to addition of 100% recommended dosages of VCI-A and VCI-B, and 50% of the recommended dosage of VCI-B. The statistical method used was Student's t-test, which is based on the hypothesis that there is no statistically significant difference between the corrosion rates used in the t-test—that is, that they are essentially identical to each other in terms of the coupon corrosion rates. The statistical result calculated by the test, P value, is the probability that the hypothesis is true. The higher the P-value, the greater the chance that the two sets of corrosion rates for the 2- and 6-month coupons are statistically similar. If the P-value is equal to or less than 0.05, it indicates that there is a less than 5% chance that the two sets of coupons have similar corrosion rates—that is, it means, with 95% confidence, that there is a statistically significant difference between the two 2- and 6-month coupons.
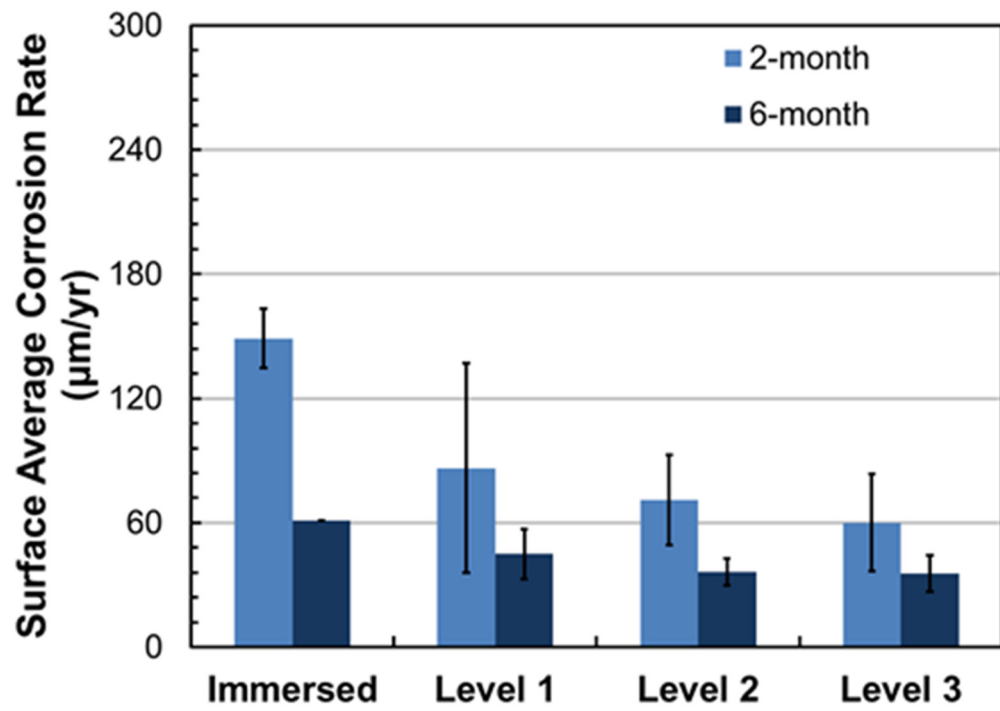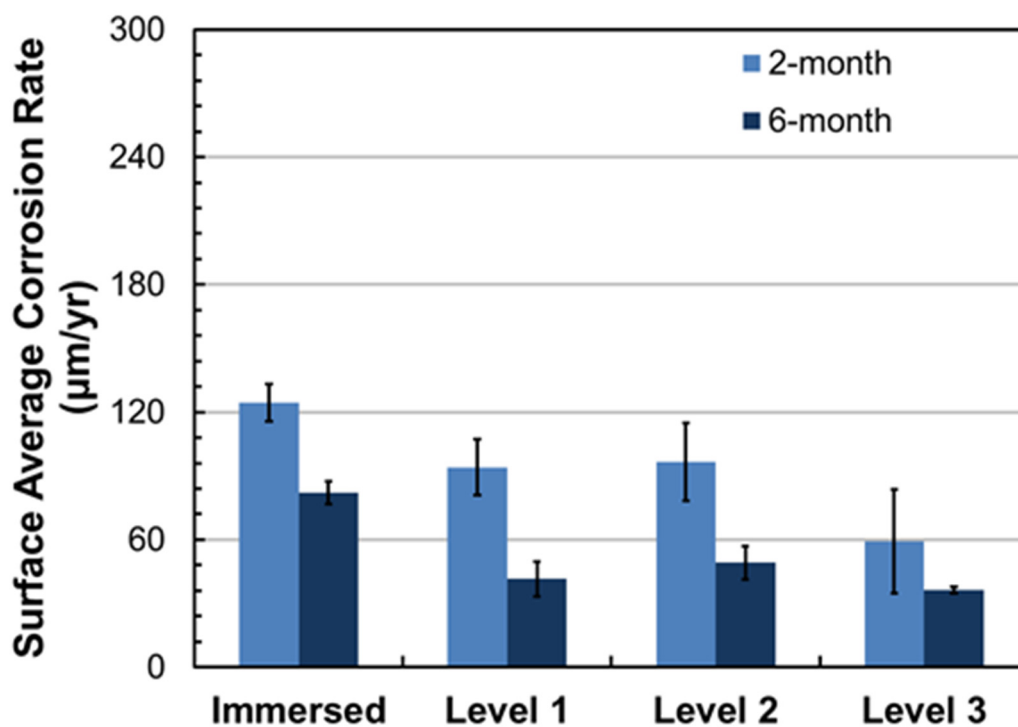
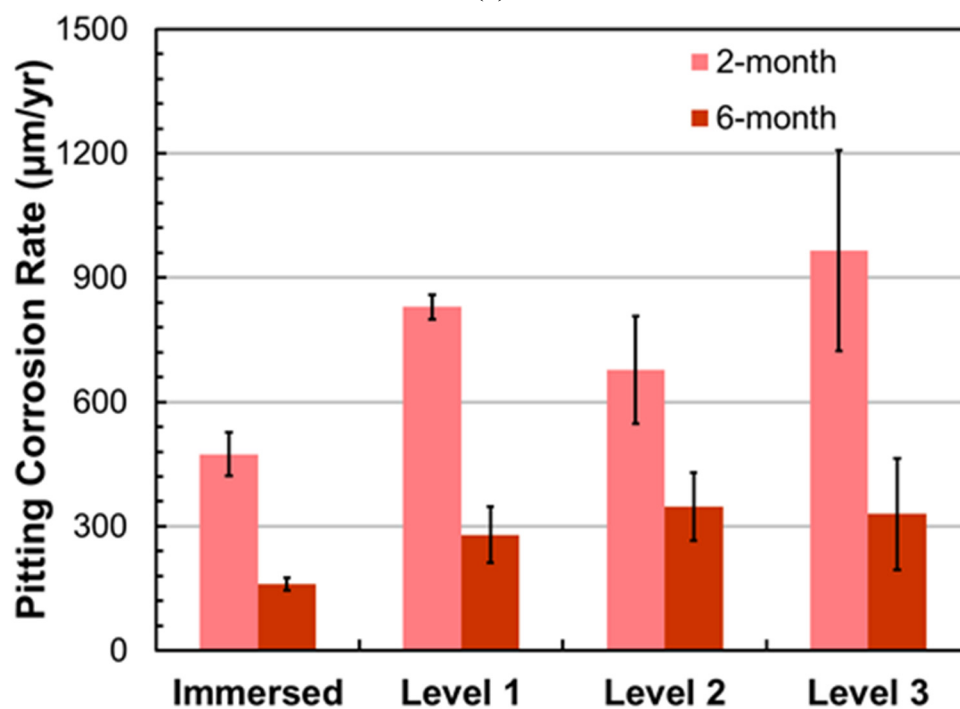(a)
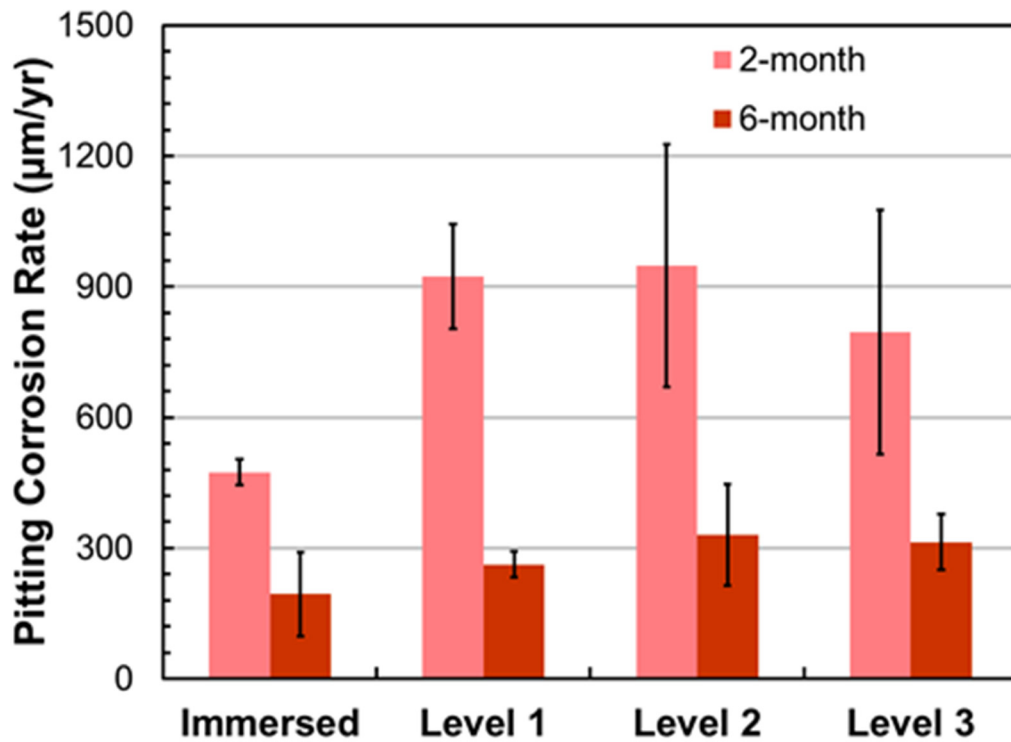
(b)

Figure 5-6. Average of (a) surface average, and (b) pitting corrosion rates for coupons in Vessel 1 (GW, and then GW +100% VCI-A). The black line in each bar represents the standard deviation.

(a)

(b)

Figure 5-7. Average of (a) surface average, and (b) pitting corrosion rates for coupons in Vessel 2. The black line in each bar represents the standard deviation.
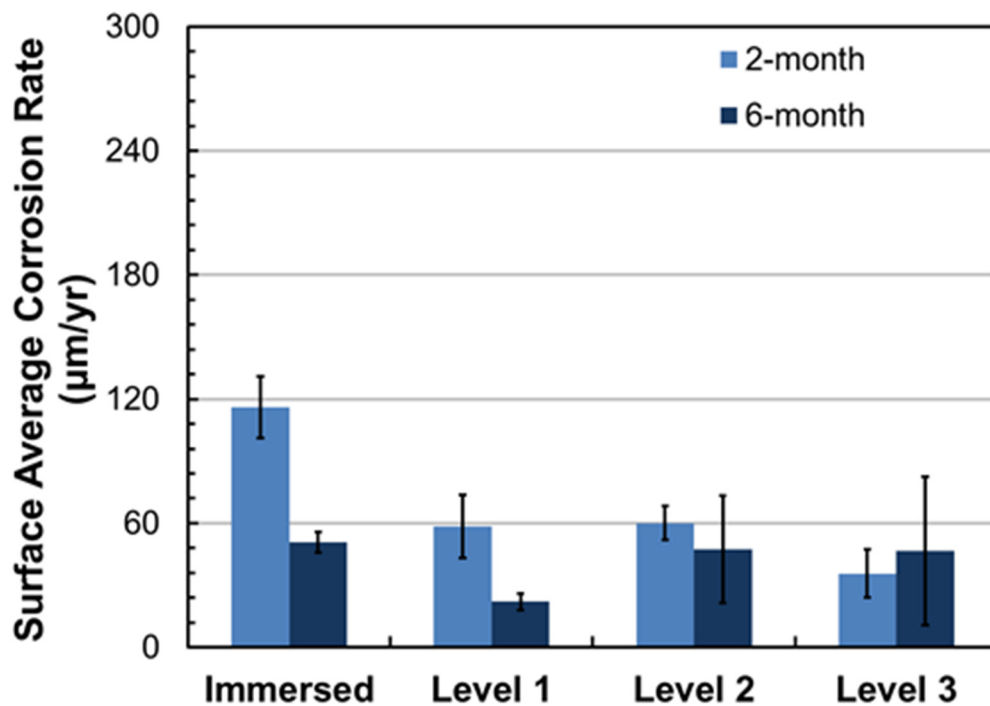
(a)

(b)

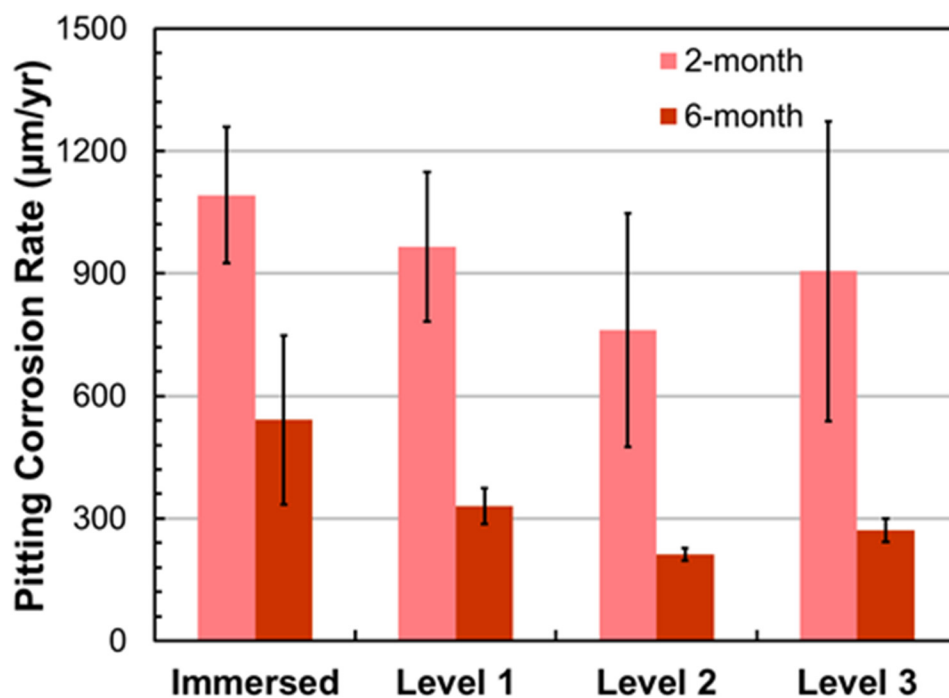**Figure 5-8. Average of (a) surface average, and (b) pitting corrosion rates for coupons in Vessel 3. The black line in each bar represents the standard deviation.**

The P-values are listed in Table 5-10. The P-values for Vessel 1 (100% VCI-A after two months) surface average corrosion rates are higher than 0.05 at Levels 1, 2, and 3, indicating that the surface average corrosion was not mitigated with 95% confidence. The large standard deviation for the 2-month surface average corrosion rate was responsible for this observation. It was noted that typically there was one coupon that produced a corrosion rate that was inconsistent with the remaining two coupons, which resulted in the large standard deviation. However, the pitting corrosion rates in Vessel 1 were mitigated in immersed, Levels 1 and 2 coupons with 95% confidence, but only with 91% confidence in Level 3 coupons.

The P-values for Vessel 2 (100% VCI-B after two months) surface average corrosion rates are lower than 0.05 for the immersed coupons, and at Levels 1 and 2, indicating that surface average corrosion rate was mitigated with 95% confidence. However, the P-value is 0.25 for the Level 3 coupons, indicating that the corrosion rate was mitigated with only 75% confidence. It is noted that the surface average corrosion rates of the 2-month Level 3 coupons fall in the range of 59 ± 24 μm/yr (2.3 ± 1 mpy) whereas the surface average corrosion rates of the 6-month Level 3 coupons are in the range of 36 ± 2 μm/yr (1.4 ± 0.07 mpy). As with VCI-A, the surface average corrosion rate for one of the 2-month coupons was significantly different than the other 2 coupons. The result was a high standard deviation, which meant that the difference between the 2- month and 6-month corrosion rates was not significant. The pitting corrosion rates in Vessel 2 were mitigated at all levels, i.e., immersed and Levels 1, 2 and 3, with 95% confidence as indicated by the P-values. This statistical analysis suggests that the performance of VCI-B is superior to that of VCI-A.

The P-values for Vessel 3 (50% VCI-B after two months) surface average corrosion rates are lower than 0.05 in immersed, and Level 1, indicating that surface average corrosion rates were mitigated with 95% confidence. However, the P-values are 0.49 and 0.66 for the Levels 2 and 3 coupons, respectively, indicating that the corrosion rates were not mitigated at Levels 2 and 3. It is noted that the surface average corrosion rates of the 2-month Level 2 coupons fall in the range of 60 ± 8 μm/yr (2.4 ± 0.3 mpy) whereas the surface average corrosion rates of the 6-month Level 3 coupons are in the range of 47 ± 26 μm/yr (1.9 ± 1.0 mpy). Similarly, the surface average corrosion rates of the 2-month Level 3 coupons fall in the range of 36 ± 12 μm/yr (1.4 ± 0.5 mpy) whereas the surface average corrosion rates of the 6-month Level 3 coupons are in the range of 47 ± 36 μm/yr (1.9 ± 1.4 mpy). In this case, variability in the 6-month corrosion rate data was responsible for the high P-value. The pitting corrosion rates in Vessel 3 were mitigated in immersed and Level 1 coupons with 95% confidence as indicated by the P-values. However, the P-values are 0.08 and 0.09 for Levels 2 and 3 coupons, respectively; these two P-values indicate that pitting corrosion is mitigated with 90% confidence. This statistical analysis suggests that the 50% dose is not as effective, however, there is some degree of mitigation particularly for the pitting corrosion.

Due to the presence of corrosion products on carbon steel surfaces, the migration rate of corrosion species to the metal surface is slowed. Thus, even without the inhibitor present, the 6-month corrosion rates would be expected to be lower than the 2-month corrosion rates. A control test, without the VCI should be performed to determine how much of reduction in rate is due to the corrosion products vs. the VCI. The control test will be performed during FY21.

**Table 5-10. Student's t-Test P-values* for Comparison Between Coupons Before and After VCI Treatment**

Corrosion Cell	Corrosion Type							
	Surface Average Corrosion				Pitting Corrosion			
	Immersed	Level 1	Level 2	Level 3	Immersed	Level 1	Level 2	Level 3
Vessel 1 (100% VCI-A)	0.01	0.29	0.10	0.20	0.03	0.01	0.05	0.09
Vessel 2 (100% VCI-B)	0.00	0.01	0.03	0.25	0.01	0.00	0.03	0.03
Vessel 3 (50% VCI-B)	0.01	0.05	0.49	0.66	0.02	0.02	0.08	0.09

*P-values of 0.05 or less indicate statistically significant differences with 95% confidence (in green). Values in red represent P-values higher than 0.05.

Vessels 1, 2 and 3 also had ER probes. In Vessels 1 and 2, the ER probes were immersed, and positioned at Levels 1 through 3. In Vessel 3, the ER probes were positioned at Levels 2 and 3. The ER probes metal loss data for Vessel 1 is presented in Figure 5-9(a). Similarly, the ER probe metal loss data for Vessels 2 and 3 are presented in Figure 5-9 (b) and Figure 5-9 (c), respectively. As seen in Figure 5-9, the ER probe data were collected using different data loggers, referred to as Model A and Model B for simplicity. The first 18-days data were collected using Model-A datalogger, at which time the Model A datalogger malfunctioned. Therefore, the Model B datalogger was used for about 40 days. The Model A datalogger was repaired and data collection began on day 77 of the experiments. The data collected using the two dataloggers are marked in Figure 5-9. The Model B data were found to be erratic and inconsistent, and therefore, were not used to estimate corrosion rates. The Model A data were used to estimate 2-month corrosion rates. The Model A data were also used to estimate the probes' corrosion rates during VCI treatment. The ER probe data during the VCI treatment were continuously collected. The probes' data were found to fluctuate between measurements. Considering this, daily, 3-period, and 5-period rolling averages of the ER probe data were calculated.

For Vessel 1, the ER probe data collected using the Model A datalogger during the VCI treatment is presented in Figure 5-10(a), Figure 5-10 (b), Figure 5-10 (c), and Figure 5-10 (d) for immersed, Level 1, Level 2, and Level 3 probes, respectively; the data in each of the four figures also include corrosion rates estimated using the 5-period rolling average of the ER probes' data. The 2-month and 6-month (for VCI treatment only) ER-probe-derived corrosion rates are listed in Table 5-11. A parallel treatment was applied to Vessels 2 and 3 ER probe data, and the coupons' and ER probes' corrosion rates are listed in Table 5-11. Vessel 2 ER probes' processed data and corresponding 5-period-rolling-average-derived corrosion rates are presented in Figure 5-11(a), Figure 5-11 (b), Figure 5-11 (c), and Figure 5-11 (d) for immersed, Level 1, Level 2, and Level 3 probes, respectively. Similarly, Vessel 3 ER probes' processed data and corresponding 5-period-rolling-average-derived corrosion rates are presented in Figure 5-12(a) and Figure 5-12 (b) for Level 2 and Level 3 probes, respectively.
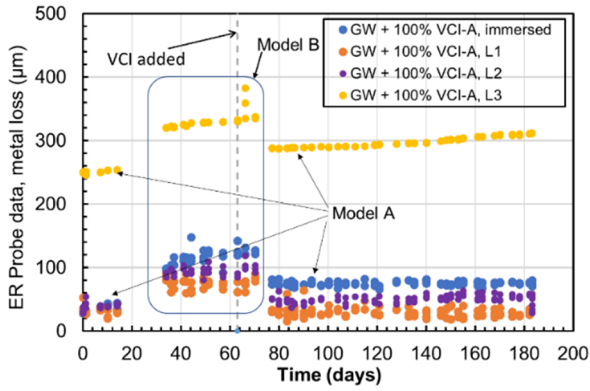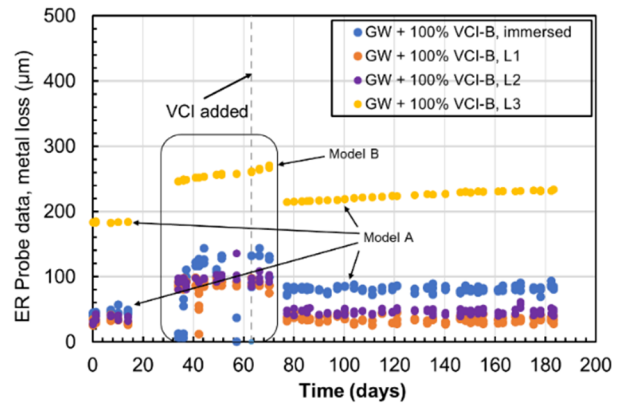
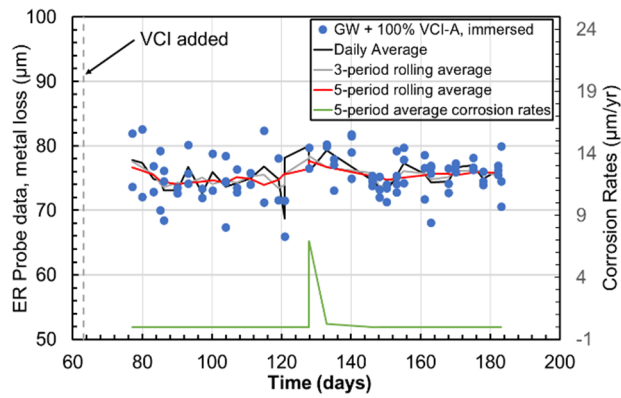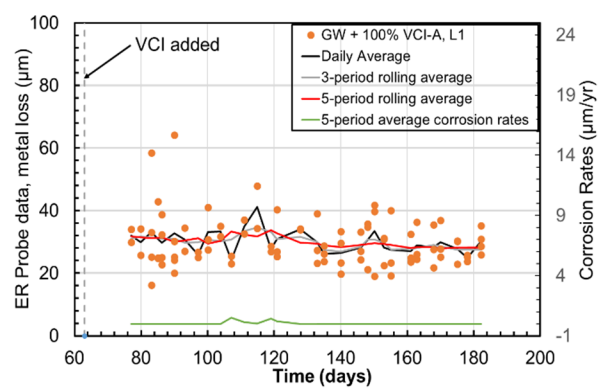(a) Vessel 1 ER probe data   (b) Vessel 2 ER probe data
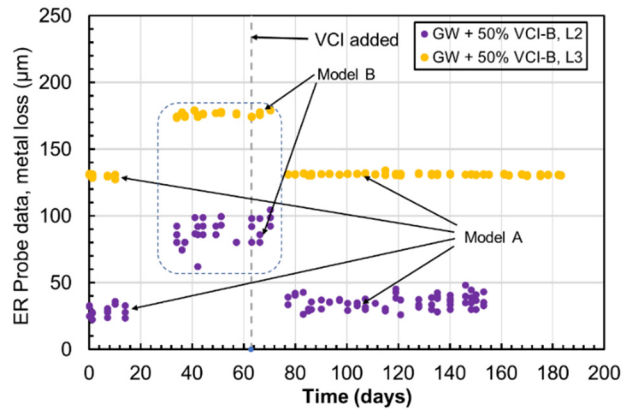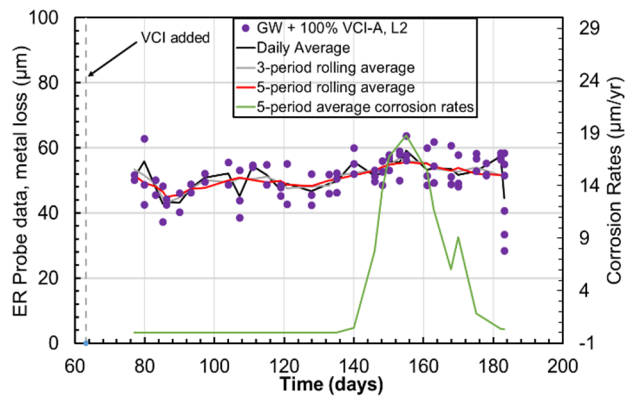
(c) Vessel 3 ER probe data

Figure 5-9. ER probes' metal loss data for the Vessels 1, 2, and 3

(a) Immersed level ER probe data and corrosion rates

(b) Level 1 ER probe data and corrosion rates

(c) Level 2 ER probe data and corrosion rates

(d) Level 3 ER probe data and corrosion rates

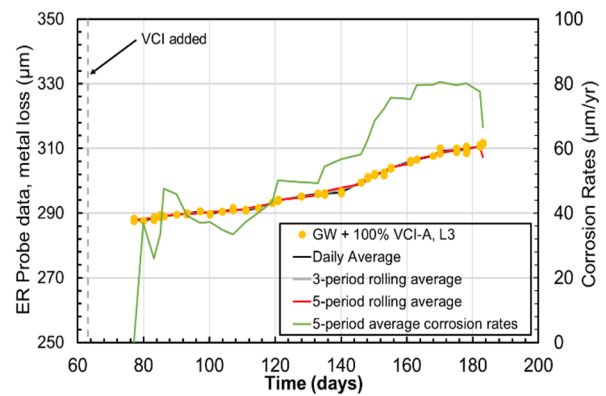**Figure 5-10. Vessel 1 ER probe data and corresponding corrosion rates**

(a) Immersed level ER probe data and corrosion rates

(b) Level 1 ER probe data and corrosion rates

(c) Level 2 ER probe data and corrosion rates

(d) Level 3 ER probe data and corrosion rates

Figure 5-11. Vessel 2 ER probe data and corresponding corrosion rates
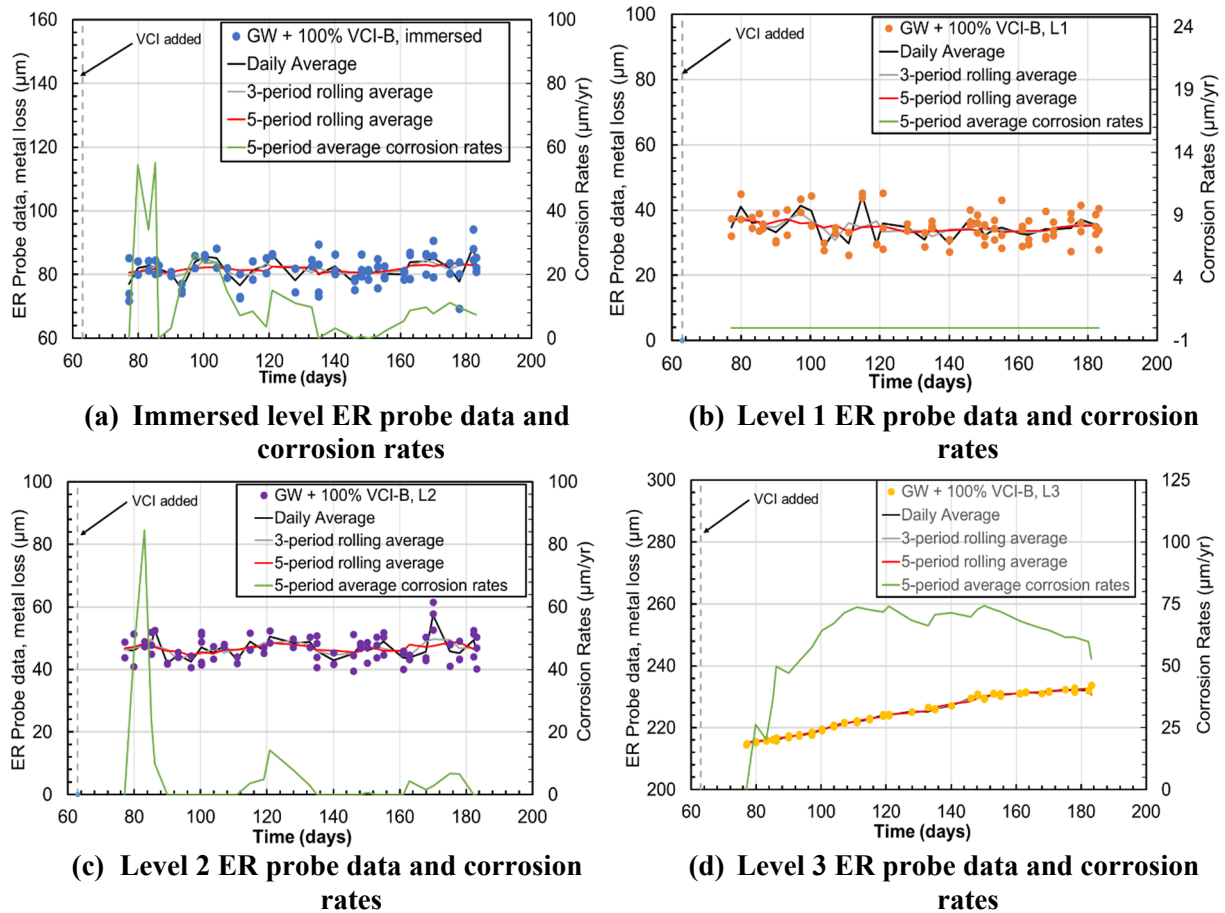

(a) Level 2 ER probe data and corrosion rates

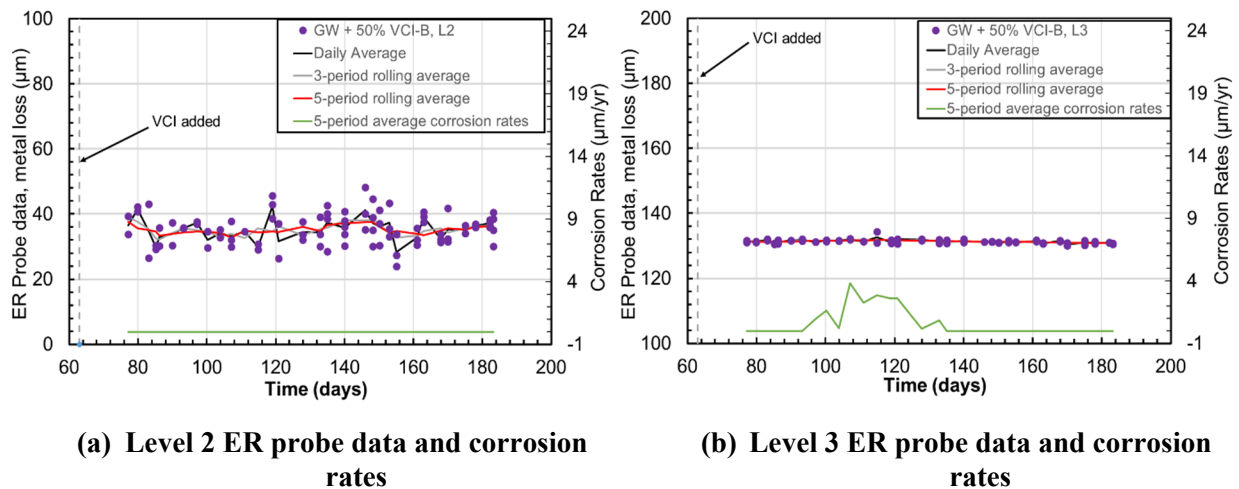(b) Level 3 ER probe data and corrosion rates

Figure 5-12. Vessel 3 ER probe data and corresponding corrosion rates

Table 5-11. Coupon and electrical resistance probe corrosion rates

Vessel	Level	Coupon Corrosion Rates (µm/yr)***		ER Probe Corrosion Rates (µm/yr)			
				3-period rolling average		5-period rolling average	
		2-month*	6-month**	2-month*	6-month♣	2-month*	6-month♣
1	Immersed	149 ± 14	61 ± 0	224	0	224	0
	Level 1	86 ± 51	45 ± 12	–	2.4	–	1.4
	Level 2	71 ± 22	36 ± 6	66	2.5	66	0.3
	Level 3	60 ± 24	36 ± 9	197	81	197	67
2	Immersed	125 ± 9	82 ± 5	207	0.5	207	7.5
	Level 1	94 ± 13	42 ± 8	15	0	15	1.7
	Level 2	97 ± 18	49 ± 8	60	2.4	60	0
	Level 3	59 ± 24	36 ± 2	147	61	147	53
3	Immersed	116 ± 15	51 ± 5	–	–	–	–
	Level 1	58 ± 15	22 ± 4	–	–	–	–
	Level 2	60 ± 8	47 ± 26	37	1.8	37	0
	Level 3	36 ± 12	47 ± 36	7	0	7	0

*2-month coupons were exposed to GW only
**6-month coupons were exposed to GW for the first two months and then to GW plus VCI for additional four months
***Corrosion rate data is estimated using three coupons per exposure level, 25 µm/yr = 1 mil/yr = 1 mpy
♣Corrosion rates are for the duration of the VCI treatment

The coupon and ER probe data were analyzed for cross consistency and to evaluate the effectiveness of VCIs in mitigating corrosion. All coupons were exposed to GW for the first two months, and only half of the coupons were extracted when VCIs were added mid-course. The remaining coupons were exposed to GW + VCI for an additional four months. The corrosion rates of the GW + VCI exposed coupons, i.e., 6-month coupons, are expected to be at least one third of the GW only exposed coupons, i.e., 2-month coupons. Ratios of the 2-month to 6-month coupons' corrosion rates were calculated; for each VCI treatment and ER probe location, two ratios were calculated using the following equation:

$$Ratio\ 1 = \frac{(Corrosion\ Rate - Std)_{2-month}}{(Corrosion\ Rate + Std)_{6-month}} \qquad Ratio\ 2 = \frac{(Corrosion\ Rate + Std)_{2-month}}{(Corrosion\ Rate - Std)_{6-month}} \qquad (1)$$

where *Ratio* 1 and *Ratio* 2 represent lower and upper bounds of the ratio range. The calculated ratio range, 6-month ER probe corrosion rates, and corrosion notes are listed in Table 5-12. If the ratio range includes a number 3 or the upper bound is close to number 3, or the ER probe corrosion rates are zero or close to zero is consistent with the corrosion rate data measured from the weight loss coupons.

Table 5-12. Ratio analysis of coupon corrosion rates and comparison with electrical resistance probe corrosion rates

Vessel	Level	Ratio of 2-month to 6-month coupon corrosion rates	6-month ER probe corrosion rates during VCI treatment* (μm/yr)	Notes
Vessel 1 (GW for first two months, and GW+100% VCI-A for additional four months)	Immersed	2.2 to 2.7	0	Ratio range upper limit is close to 3
	Level 1	0.6 to 4.2	1.4	Ratio range includes 3
	Level 2	1.1 to 3	0.3	Ratio range includes 3
	Level 3	0.8 to 3	67	Ratio range include 3, but ER probe corrosion rates were high
Vessel 2 (GW for first two months, and GW+100% VCI-B for additional four months)	Immersed	1.3 to 1.8	7.5	Ratio range does not include 3
	Level 1	1.6 to 3.1	1.7	Ratio range includes 3
	Level 2	1.4 to 2.8	0	Ratio range upper limit is close to 3
	Level 3	0.9 to 2.5	53	Ratio range upper limit is close to 3
Vessel 3 (GW for first two months, and GW+50% VCI-B for additional four months)	Level 2	0.7 to 3.2	0	Ratio range includes 3
	Level 3	0.3 to 4.4	0	Ratio range includes 3
*VCI treatment only corrosion rates based on 5-period rolling average				

The Vessel 1 ER-probe-derived corrosion rates are consistent with coupons' corrosion rates in immersed, Level 1, and Level 2, as listed in Table 5-12. However, Level 3 ER-probe-derived corrosion rate was found to be not consistent with the coupons' corrosion rate. This may be due to the wire element probe that was used at Level 3. The thinness and surface area of the wire probe element was much smaller compared to the cylindrical probes that were used in immersed, Level 1, and Level 2.

The Vessel 2 ER-probe-derived corrosion rates are consistent with coupons' corrosion rates at Level 1 and Level 2, as listed in Table 5-12. The corrosion rate ratio for the immersed coupons range between 1.3 to 1.8, and the ER-probe-derived corrosion rate is 7.5 μm/yr. The ER probe corrosion rate needed to be at least 33 μm/yr to be consistent with the coupons' corrosion rate. Similarly, the ER-probe-derived corrosion rate at Level 3 were not consistent with the coupons' corrosion rates; the ER-probe rate was 53 μm/yr but needed to be approximately 15 μm/yr to be consistent with coupons' corrosion rates. The use of wire-element probe may have skewed the data at Level 3 because wire element surface area may not have been sufficiently large to accumulate enough VCI needed for corrosion mitigation.

The Vessel 3 ER-probe-derived corrosion rates are consistent with coupons' corrosion rates at Level 2 and Level 3, as listed in Table 5-12. The corrosion rates' ratio ranges for both Levels 2 and 3 included 3, and ER-probe derived corrosion rates were zero. Overall, the cylindrical probe elements were used at six locations, and of those, five of them reported the corrosion rates that were consistent with the coupons'

corrosion rates. However, the wire-element probes were used at three locations, and only one location's ER probe data were consistent with the coupons' data.

5.5 <u>Long Term OCP Drift</u>

The OCP data for the bullet, mill-scale, and partial mill-scale coupons were collected for several months. A summary of the initial and final potential data is shown in Table 5-13. The data for the coupons exposed to AY-101 are presented in Figure 5-13; initial OCPs of the bullet, mill-scale, and partial mill-scale coupons are -557, -176, and -388 mV$_{SCE}$, respectively. The potentials of the three electrodes quickly evolved and eventually settled to approximately -140 mV$_{SCE}$ for the bullet, mill-scale, and partial mill-scale coupons after four months of evolution; this indicated that terminal OCPs are independent of the surface condition in AY-101 simulant.

The OCP data for the three coupons in SY-101 simulant are presented in Figure 5-14. Initial OCPs of the bullet, mill-scale, and partial mill-scale coupons are -492, -183, and -323 mV$_{SCE}$, respectively. In the first 500 hours, the potentials of the three electrodes quickly evolved, however, the rate of evolution became slow thereafter. The OCPs of the electrode after 4000 hours are as follows: -74 mV$_{SCE}$, -298 mV$_{SCE}$, and -340 mV$_{SCE}$ for the bullet, mill-scale, and partial mill-scale coupons. As seen in Figure 5-14, the potentials continued to evolve even after 4000 hours of exposure and did not reach steady state. The potentials of the partial mill-scale coupon suddenly shifted to more-negative values after 2300 hours, as seen in Figure 5-14; this shift caused the potentials of the mill-scale and partial mill-scale coupons to be close to each other, and thus potentials of the two electrodes were at least 200 mV more cathodic than the polished surface, i.e., bullet coupon. The reason for the decrease is unknown, however, both the mill-scale and partial mill scale were at approximately the same value as the initial value for the actual tank potential and the average value of the tank potential. It is not known if the potential for the laboratory tests would have stabilized or continued to decrease.

The OCP data for the three coupons in AW-105 Base are presented in Figure 5-15. Initial OCPs of the bullet, mill-scale, and partial mill-scale coupons are -668, -284, and -405 mV$_{SCE}$, respectively. In the first 500 hours, the potentials of the three electrodes quickly evolved, however, the rate of evolution became slow thereafter. The OCPs of the electrode after 4000 hours are -256 mV$_{SCE}$, -186 mV$_{SCE}$, and -319 mV$_{SCE}$ for the bullet, mill-scale, and partial mill-scale coupons, respectively. .

The OCP data for the bullet and mill-scale coupons in AW-105 Representative simulant are presented in Figure 5-16. Initial OCPs of the bullet and mill-scale coupons are -516 and -205 mV$_{SCE}$, respectively. In the first 10 hours, the potentials of the two coupons quickly evolved. The OCPs of the electrode after 1200 hours are following: -239 mV$_{SCE}$ and -251 mV$_{SCE}$ for the bullet and mill-scale coupons, respectively.

Table 5-13. Summary of OCP (mV$_{SCE}$) data

Simulant	Bullet		Mill-Scale		Partial Mill-Scale	
	Initial	After	Initial	After	Initial	After
AY-101	-557	-140	-175	-140	-388	-140
SY-101	-492	-73	-183	-304	-324	-333
AW-105 Base)	-668	-256	-284	-201	-405	-319
AW-105 Representative	-516	-236	-205	-240	–	–
AW-105 Elevated TOC	-893	-461	-300	-435	-299	-573
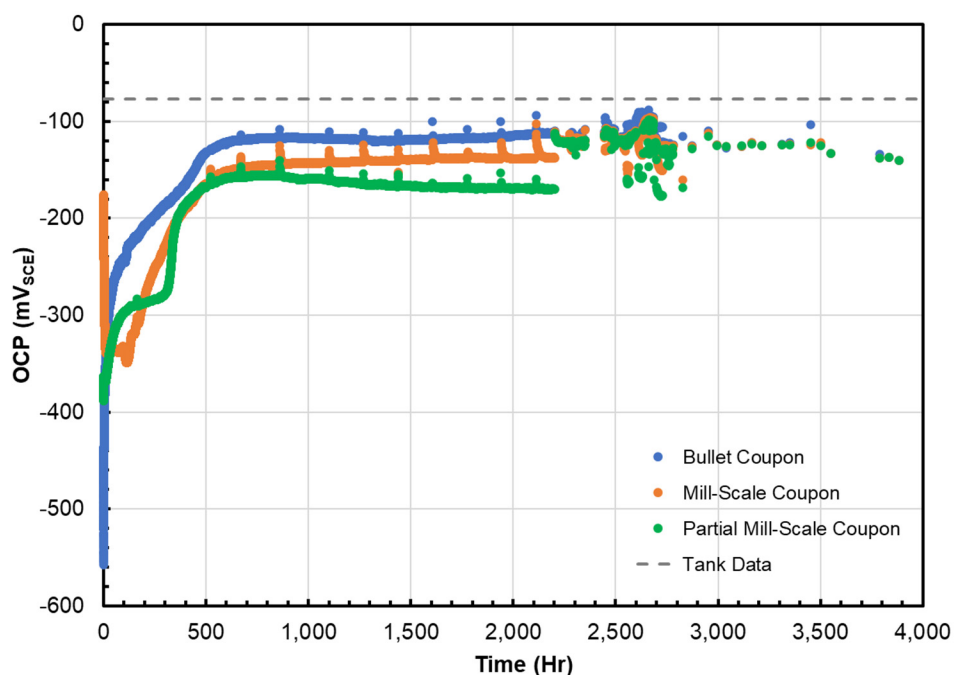
Figure 5-13. OCP data for the bullet (600-grit polished surface), mill-scale, and partial mill-scale coupons in AY-101 simulant.   The tank data represents the average open circuit potential over 0.5 years. Note that the initial tank potential for the first 3 months was -80 mV vs. SCE.
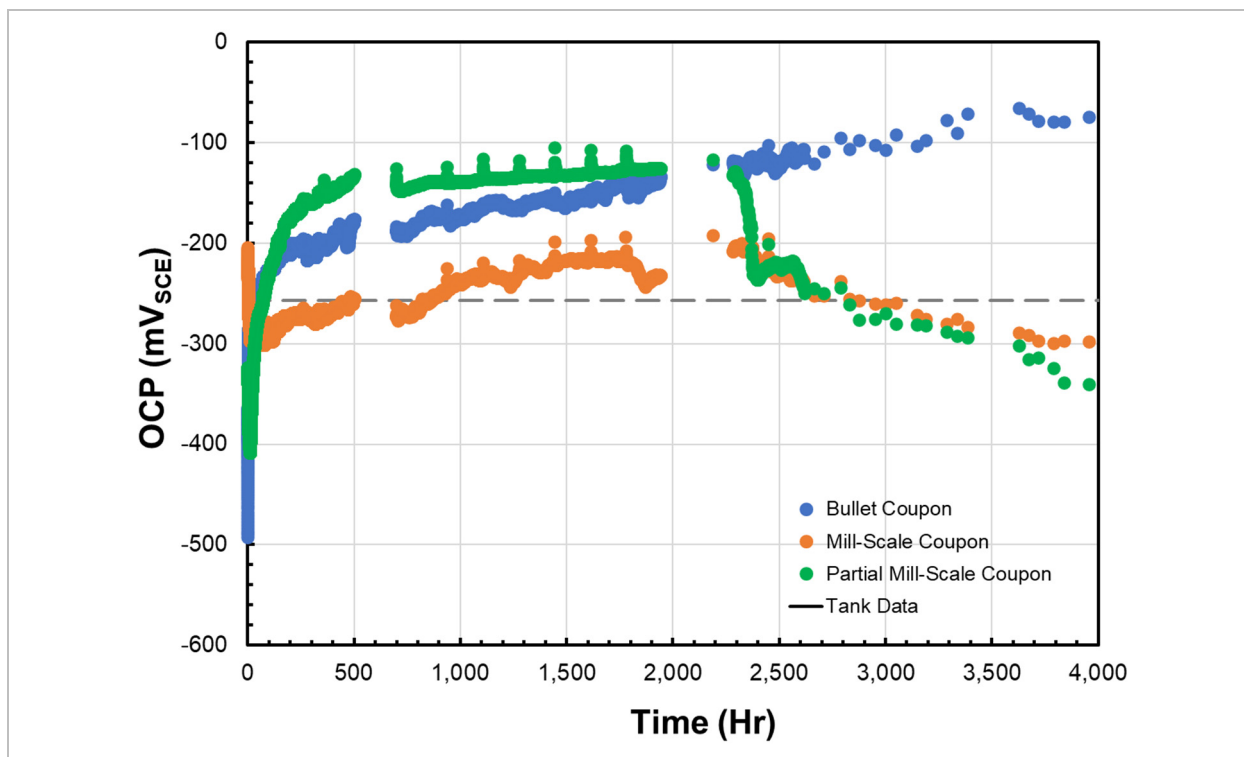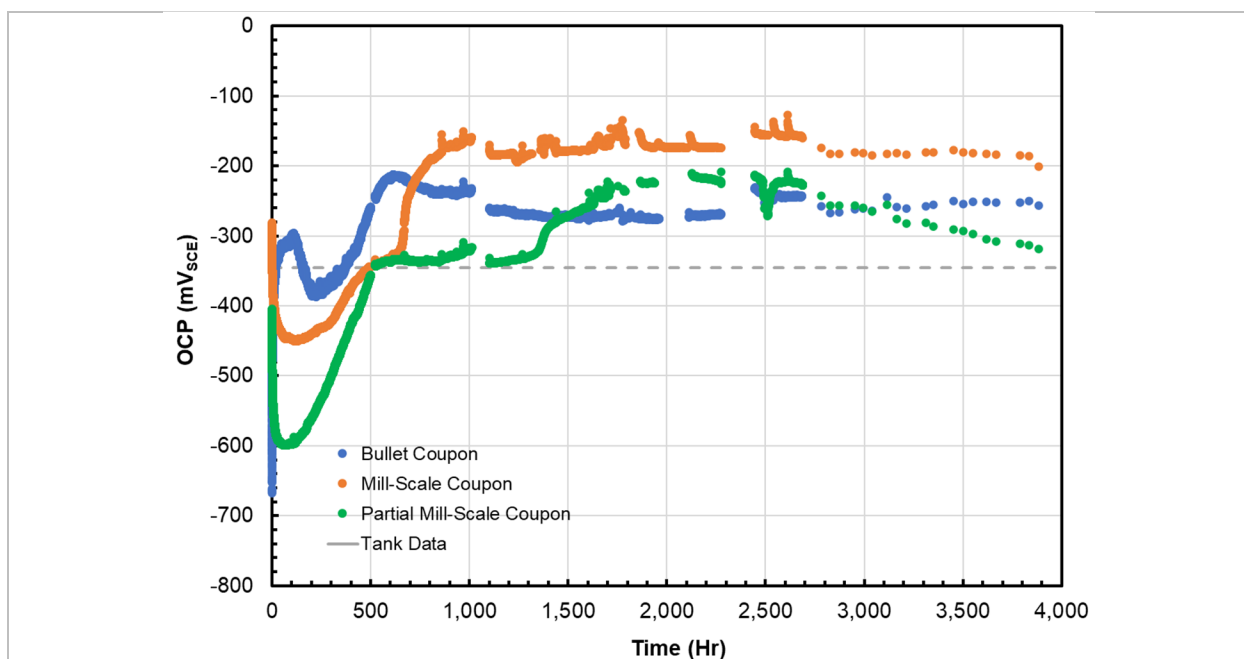
Figure 5-14. OCP data for the bullet (600-grit polished surface), mill-scale, and partial mill-scale coupons in SY-101 simulant.   The tank data represents the average open circuit potential over 5.5 years. Note that the initial tank potential for the first 3 months was -257 mV vs. SCE.

Figure 5-15. OCP data for the bullet (600-grit polished surface), mill-scale, and partial mill-scale coupons in AW-105 Base.   The tank data represents the average open circuit potential over 6.5 years. Note that the initial tank potential for the first 3 months was -257 mV vs. SCE.

Figure 5-16. OCP data for the bullet (600-grit polished surface) and mill-scale coupons in AW-105 Representative simulant. The tank data represents the average open circuit potential over 6.5 years. Note that the initial tank potential for the first 3 months was -257 mV vs. SCE.
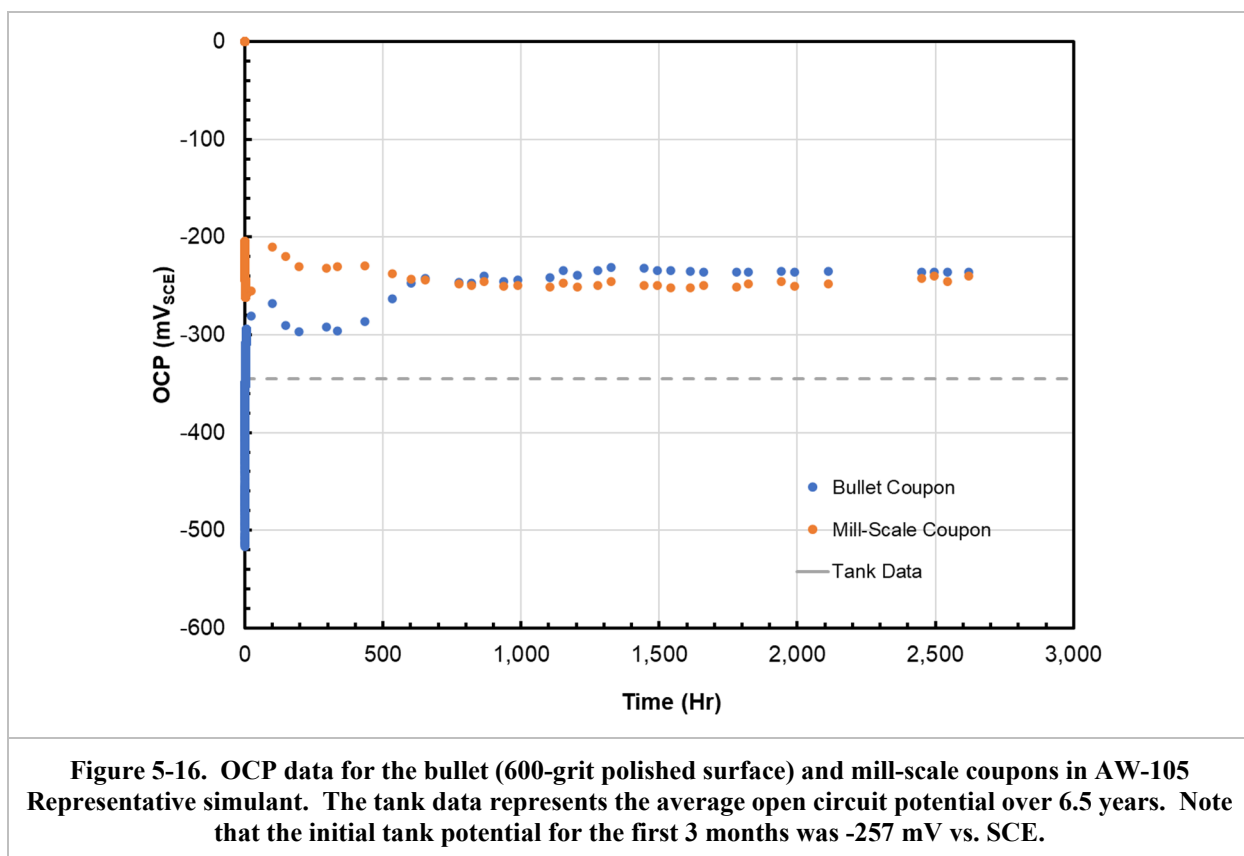
The OCP data for the three coupons in AW-105 Elevated TOC simulant are presented in Figure 5-17. Initial OCPs of the bullet, mill-scale, and partial mill-scale coupons are -893, -300, and -299 mV$_{SCE}$, respectively. In the first 100 hours, the potentials of the three electrodes quickly evolved, however, the rate of evolution became slow thereafter. The OCPs of the coupons after 2350 hours are following: -494 mV$_{SCE}$, -459 mV$_{SCE}$, and -480 mV$_{SCE}$ for the bullet, mill-scale, and partial mill-scale coupons.

Figure 5-13 to Figure 5-17 also contain the average actual tank data, which are represented by gray dashed line in each figure. The caption for the figure also includes the actual tank data that were obtained for the first three months. The tank data are listed in Table 5-14. The initial and the last OCPs are listed in Table 5-13. The tank and simulant OCP data were analyzed, and analysis results are presented in Table 5-15.
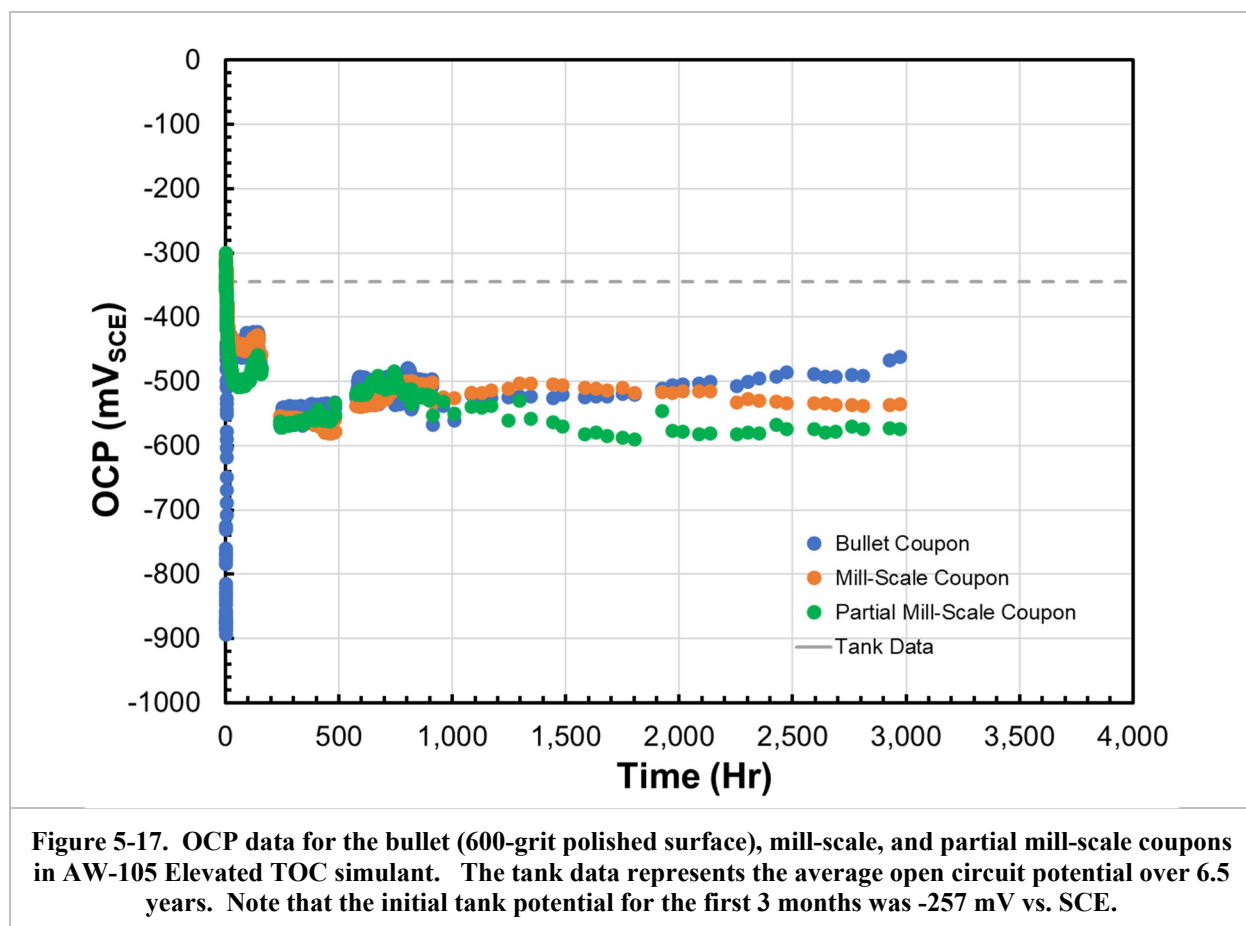
Figure 5-17. OCP data for the bullet (600-grit polished surface), mill-scale, and partial mill-scale coupons in AW-105 Elevated TOC simulant. The tank data represents the average open circuit potential over 6.5 years. Note that the initial tank potential for the first 3 months was -257 mV vs. SCE.

Table 5-14. OCP (mV$_{SCE}$) Data of Tanks

Tank	Years of Service	Initial Potential (mV$_{SCE}$)	Final Potential (mV$_{SCE}$)	Average Potential (mV$_{SCE}$)	Std. Dev. (mV$_{SCE}$)
AY-101	0.5	-80	-74	-77	NA
SY-101	5.5	-257	-279	-257	13
AW-105	6.5	-253	-394	-345	78

Table 5-15. Comparison of tank wall and simulant OCP data

Tank	Tank-Wall OCP	Simulant OCP Data and Notes
AY-101	-77 mV$_{SCE}$	• -140 mV$_{SCE}$ for all three coupons; simulant OCPs are -63 mV more cathodic than the tank-wall OCP
SY-101	-257 ± 13 mV$_{SCE}$ (-244 to -270 mV$_{SCE}$)	• -73 mV$_{SCE}$, -298 mV$_{SCE}$, and -340 mV$_{SCE}$ for the bullet, mill-scale, and partial mill-scale coupons, respectively • Mill-scale coupon's OCP are closest to the average and the initial tank tank-wall potential
AW-105	-345 ± 78 mV$_{SCE}$ (-267 to -423 mV$_{SCE}$)	AW-105 Base • -201 mV$_{SCE}$, -256 mV$_{SCE}$, and -319 mV$_{SCE}$ for the bullet, mill-scale, and partial mill-scale coupons, respectively • Partial mill-scale coupon's OCP is within the tank-wall OCP range • Mill-scale and bullet coupons' OCPs are close to the tank potential
		AW-105 Representative • -239 mV$_{SCE}$ and -251 mV$_{SCE}$ for the bullet and mill-scale coupons, respectively • Both bullet and mill-scale coupons' OCPs are near the range, within 30 mV of the initial tank potential data
		AW-105 Elevated TOC • -461 mV$_{SCE}$, -535 mV$_{SCE}$, and -573 mV$_{SCE}$ for the bullet, mill-scale, and partial mill-scale coupons, respectively • Coupons' OCPs are outside the range of the actual tank data.

EIS measurements were conducted in the frequency range of 10^4 to 10^{-4} Hz, immediately after completing the OCP measurements. EIS data for the coupons in the AY-101 and SY-101 simulants are presented in Figure 5-18.
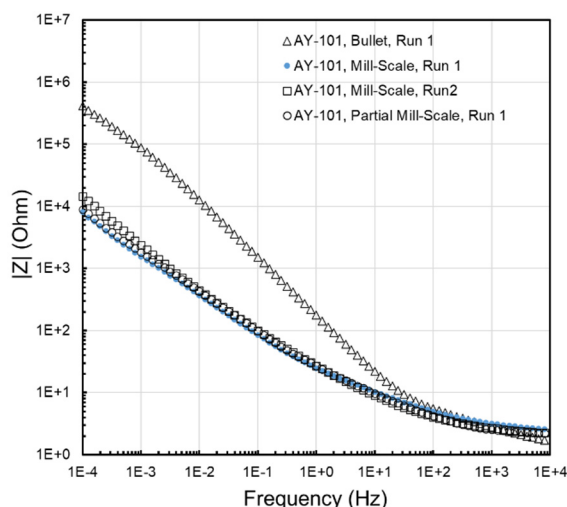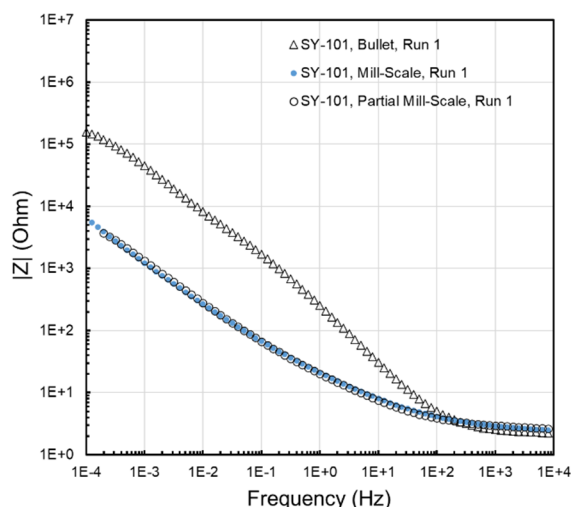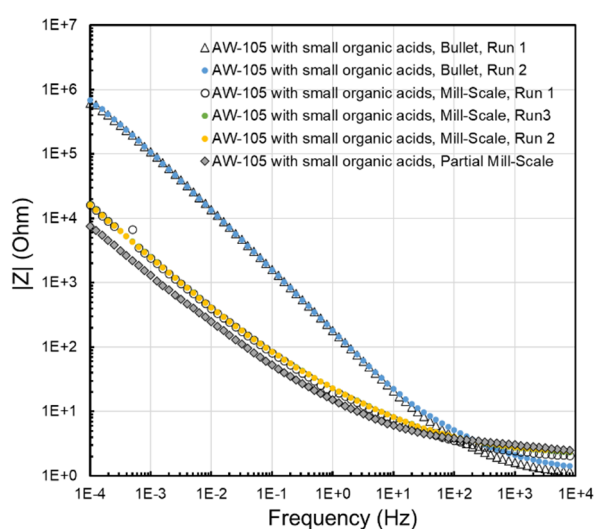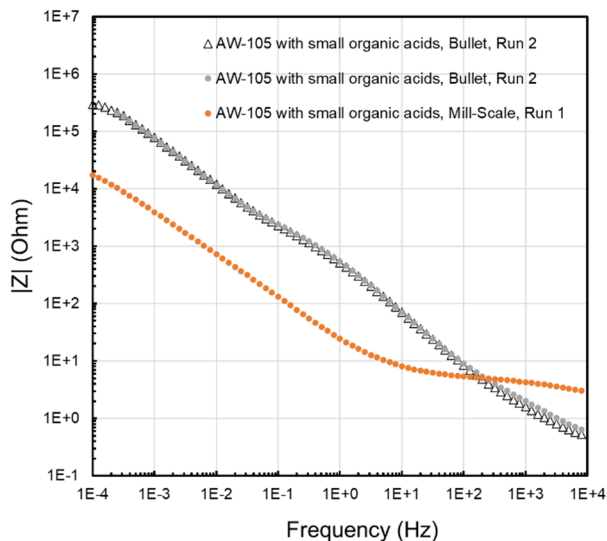

(a) AY-101	**(b) SY-101**

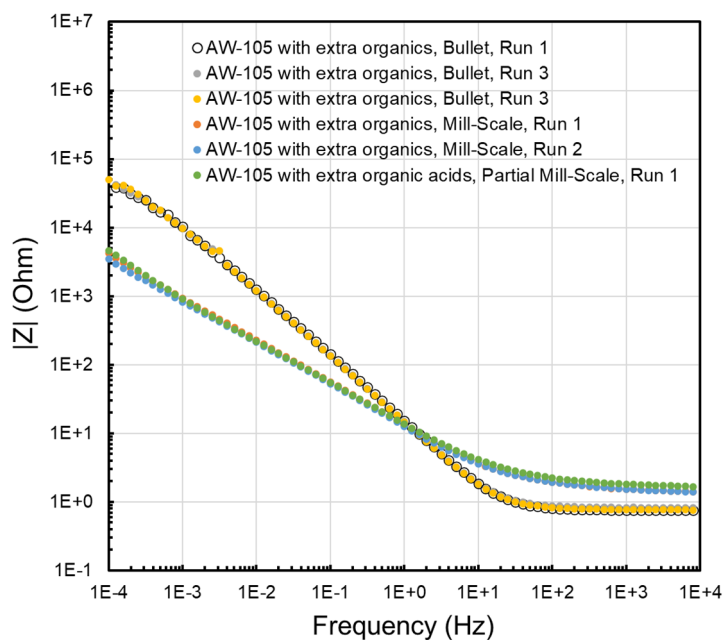**Figure 5-18: EIS data for bullet, mill-scale, and partial mill-scale coupons in AY-101 and SY-101.**

EIS data for the bullet, mill-scale, and partial mill-scale coupons in AW-105 Base and AW-105 Representative are presented in Figure 5-19(a) and Figure 5-19(b), respectively. EIS data for the bullet and mill-scale coupons in AW-105 Elevated TOC are presented in Figure 5-19(c).

(a) AW-105 Base

(b) AW-105 Representative

(c) AW-105 Elevated TOC

Figure 5-19. EIS data for bullet, mill-scale, and partial mill-scale coupons in the three variants of AW-105 simulants.

The following observations were made for the impedance spectra of the coupons:
- Even at the low-end frequency spectra of the both sets of coupons, the asymptotic impedance values could not be measured, indicating that charge transfer resistances associated with the metal interface reactions are higher than the lowest frequency impedance values.
- Impedance spectra of the coupons in AY-101, SY-101, AW-105 Base, and AW-105 Elevated TOC exhibited a single time-constant type response, indicating that activation-control reaction kinetics is dominant for the three electrodes. Impedance spectra of the bullet coupon in AW-105 Representative exhibited a two time-constant response, but the mill-scale coupon exhibited only a one-time constant response.
- Low frequency impedances of the mill-scale and partial mill-scale coupons were lower than bullet coupon impedance in AY-101, SY-101, and AW-105 Base. This indicates that polarization resistance of the bullet coupons in the three simulants is higher than the mill-scale and partial mill-scale coupons. This observation is also consistent with the CPP data where higher passive current densities were observed for the mill-scale and partial mill-scale coupons compared to the bullet coupons in the three simulants.

The CPP data for the bullet, mill-scale, and partial mill-scale coupons in AY-101 simulant is presented in Figure 5-20(a). The three coupons' CPP responses exhibit negative hysteresis, i.e., pitting corrosion of the electrode material is unlikely in the simulant chemistry. The passive current density of the bullet coupon is approximately 2×10^{-4} mA/cm^2. It is noted that the passive current density of the bullet coupon is about two orders of magnitude lower than the mill-scale and partial-mill coupons. There are two plausible explanation for the higher passive current densities of the mill-scale and partial mill-scale coupons: (i) there are anodic reactions other than the metal dissolution reactions that occur on the mill-scale and partial mill-scale coupons leading to higher current densities during the forward scans of the CPP curves, and (ii) the passive film that developed on the bare metal surface could not be fully developed due to presence of mill-scale and corrosion products on the mill-scale and partial mill-scale coupons. These two hypotheses require further investigation.
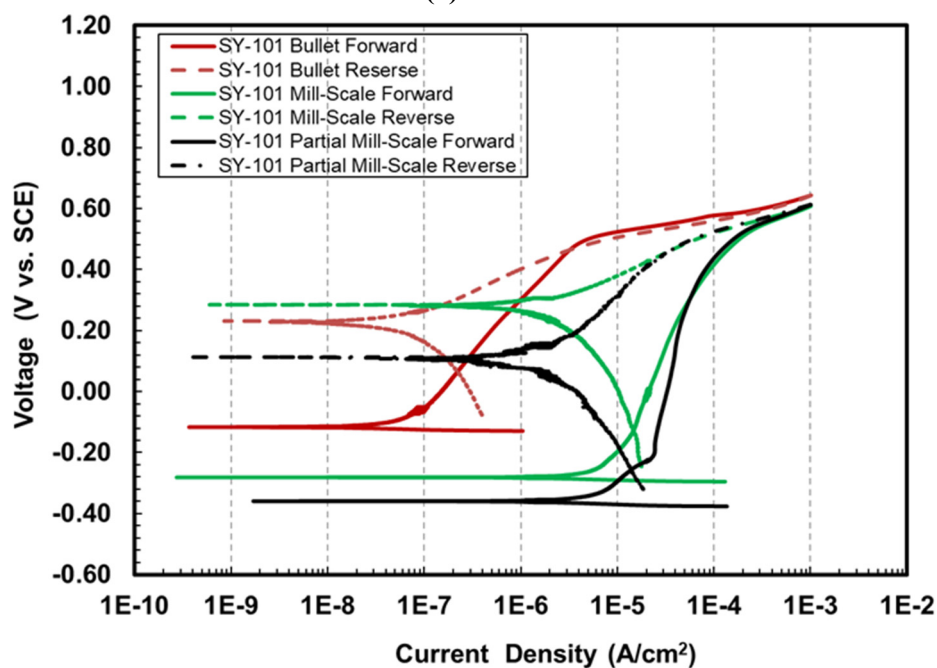
The CPP data for the bullet, mill-scale, and partial mill-scale coupons in SY-101 simulant is presented in Figure 5-20(b). The three coupons' CPP responses exhibit negative hysteresis, i.e., pitting corrosion of the electrode material is unlikely in the simulant chemistry. The passive current density of the bullet coupon is approximately 4×10^{-4} mA/cm^2. Compared to the mill-scale and partial mill-scale coupons, the passive current density of the bullet coupon is about two orders of magnitude lower. As mentioned previously, the two plausible explanations could be due to anodic reactions other than the metal dissolution on the mill-scale and corrosion product layer of the mill-scale and partial mill-scale coupons, and lack of complete passive film coverage on the mill-scale and partial mill-scale coupons.

The CPP data for the bullet, mill-scale, and partial mill-scale coupons in AW-105 Base is presented in Figure 5-21(a). The three coupons' CPP responses exhibit negative hysteresis, i.e., pitting corrosion of the electrode material is unlikely in the simulant chemistry. The passive current density of the bullet coupon is in the range of 10^{-4} to 10^{-3} mA/cm^2. Compared to the mill-scale and partial mill-scale coupons, the passive current density of the bullet coupon is about one-two orders of magnitude lower. The two plausible explanations, as mentioned previously, could be the cause of higher passive current density in the mill-scale and partial mill-scale co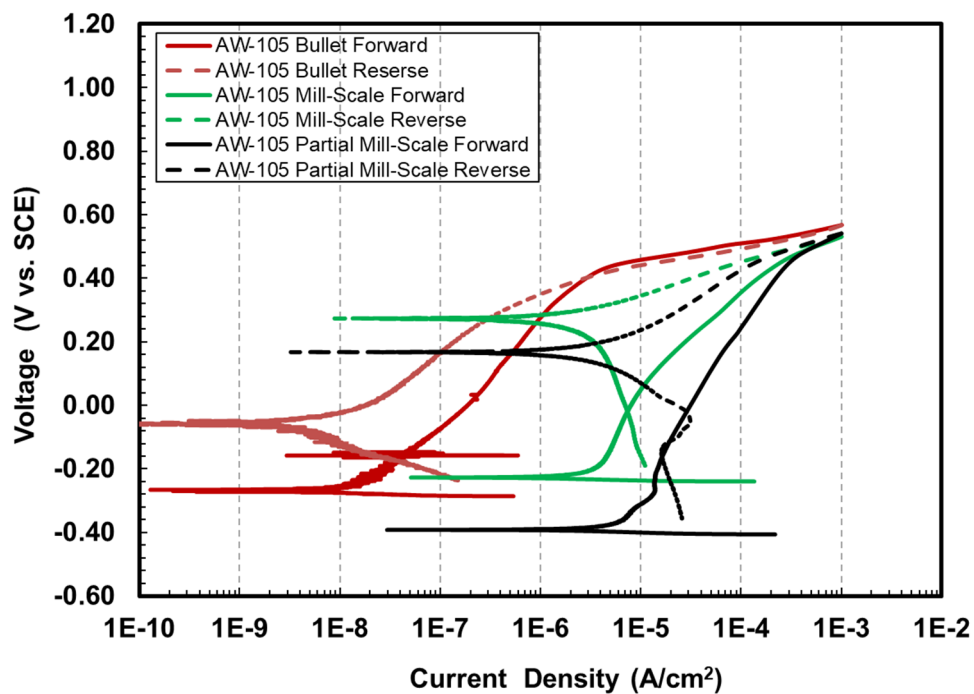upons compared to the bullet coupon. The CPP data for the bullet, mill-scale, and partial mill-scale coupons in AW-105 Representative are presented in Figure 5-21 (b). The two coupons' CPP responses exhibit negative hysteresis, i.e., pitting corrosion of the electrode material is unlikely in the simulant chemistry. The passive current density of the bullet coupon is in the range of 10^{-4} to 10^{-3} mA/cm^2. Compared to the mill-scale, the passive current density of the bullet coupon is about one-two orders of magnitude lower. The two plausible explanations, as mentioned previously, could be the

cause of higher passive current density in the mill-scale and partial mill-scale coupons compared to the bullet coupon.
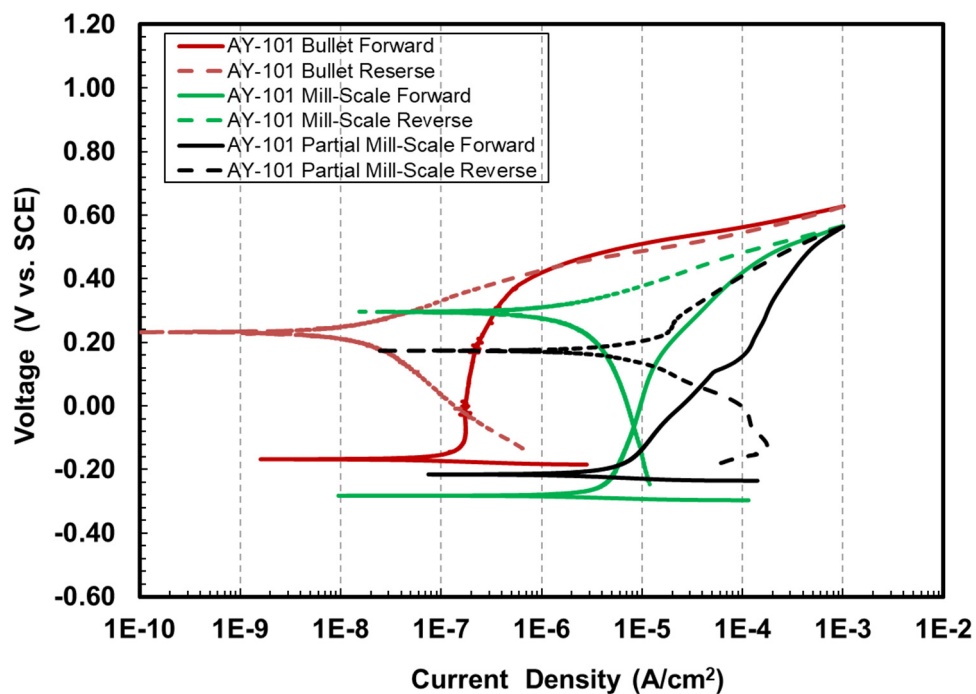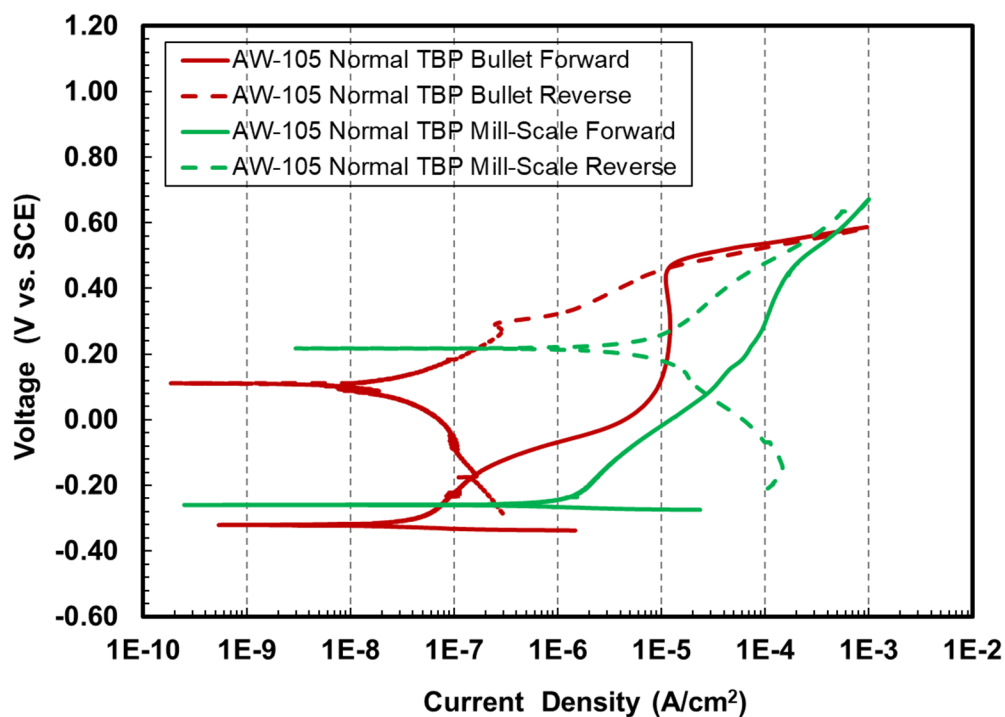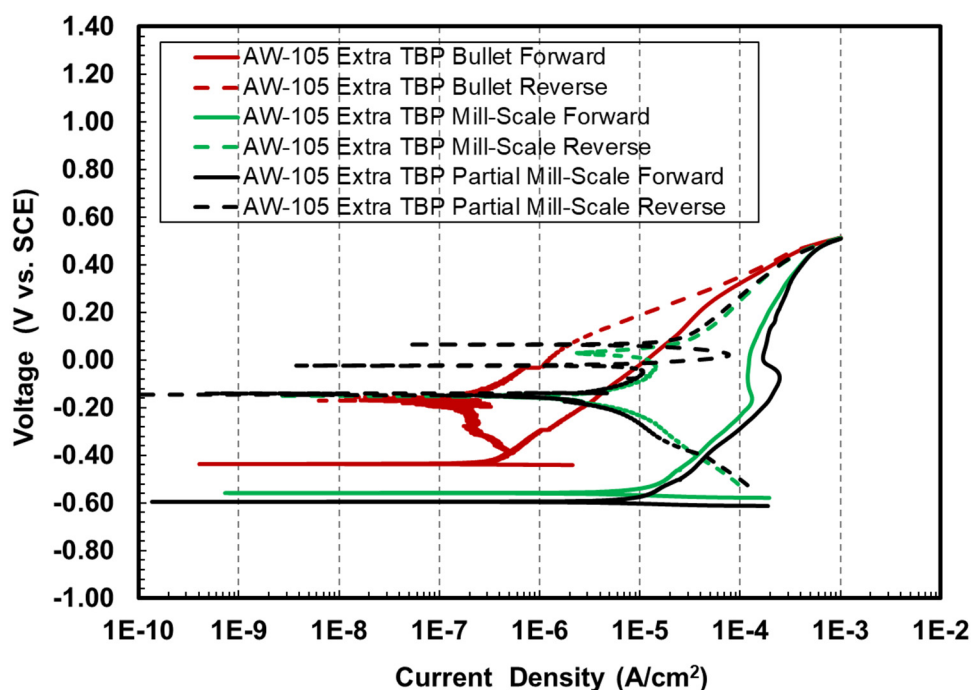

(a) AY-101

(b) SY-101

Figure 5-20. CPP data for the bullet, mill-scale, and partial mill-scale coupons after OCP holds in (a) AY-101 and (b) SY-101 simulants

(a) AW-105 Base

(b) AW-105 Representative

Figure 5-21. CPP data for (a) AW-105 Base, and (b) AW-105 Representative

The CPP data for the bullet, mill-scale, and partial mill-scale coupons in AW-105 Elevated TOC are presented in Figure 5-22. The three coupons' CPP responses exhibit negative hysteresis, i.e., pitting corrosion of the electrode material is unlikely in the simulant chemistry. The passive current density of the bullet coupon is in the range of 10^{-4} to 10^{-3} mA/cm^2. Compared to the mill-scale and partial mill-scale coupons, the passive current density of the bullet coupon is about one-two orders of magnitude lower. The two plausible explanations, as mentioned previously, could be the cause of higher passive current density in the mill-scale and partial mill-scale coupons compared to the bullet coupon.

Figure 5-22. CPP data for AW-105 Elevated TOC

Images of the coupons after OCP hold, EIS and CPP measurements are presented in Table 5-16 and Table 5-17. Images of the bullet, mill-scale, and partial mill-scale coupons in AY-101 simulant are presented in in the first row of Table 5-16. Although discoloration of the coupons did occur, no visible signs of pitting corrosion were observed on the three coupons. Similarly, images of the bullet, mill-scale, and partial mill-scale coupons in SY-101 simulant are presented in the second row of Table 5-16. No visible signs of pitting corrosions were observed in the three coupons in SY-101 simulant. In addition, discoloration of the coupons in SY-101 was not as severe as in AY-101 simulant.

Images of the bullet, mill-scale, and partial mill-scale coupons in AW-105 Base are presented in the first row of Table 5-17. Similar to AY-101 and SY-101, coupons discoloration did occur in the AW-105 Base simulant, but no visible signs of pitting corrosion were observed in the three coupons. Images of the bullet and mill-scale coupons in AW-105 Representative are presented in the second row of Table 5-17; heavy discoloration of the coupons was observed, and this was attributed to the presence or organics in the simulant. Images of the bullet, mill-scale, and partial mill-scale coupons in AW-105 Elevated TOC are shown in the third row of Table 5-17; heavy discoloration observed on the coupons was attributed to the presence or organics in the simulant. No signs of pitting were observed on any of the coupons. The CPP data is summarized in Table 5-18.

Table 5-16. Images of the coupons after exposure to AY-101 and SY-101 simulants
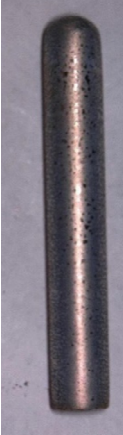
Simulant	Bullet	Mill-Scale	Partial Mill-Scale
AY-101			
SY-101			

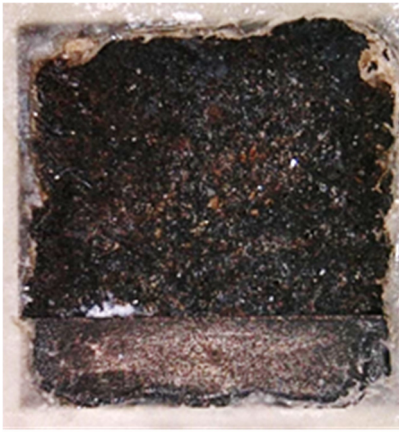**Table 5-17. Images of the coupons after exposure to the three versions of AW-105 simulants**

Simulant	Bullet	Mill-Scale	Partial Mill-Scale
AW-105 Base			
AW-105 Representative			N/A
AW-105 Elevated TOC			

Table 5-18. CPP data summary

Simulant	Bullet Coupon	Mill-Scale	Partial Mill-Scale	Notes
AY-101	Negative hysteresis, Category 1 (no pitting)	Negative hysteresis, Category 1 (no pitting)	Negative hysteresis, Category 1 (no pitting)	Mill- and partial mill-scale coupons' forward scan passive current densities are 1-2 orders of magnitude lower than the bullet coupon's forward scan passive current density
SY-101	Negative hysteresis, Category 1 (no pitting)	Negative hysteresis, Category 1 (no pitting)	Negative hysteresis, Category 1 (no pitting)	Mill- and partial mill-scale coupons' forward scan passive current densities are 1-2 orders of magnitude lower than the bullet coupon's forward scan passive current density
AW-105 Base	Negative hysteresis, Category 1 (no pitting)	Negative hysteresis, Category 1 (no pitting)	Negative hysteresis, Category 1 (no pitting)	Mill- and partial mill-scale coupons' forward scan passive current densities are 1-2 orders of magnitude lower than the bullet coupon's forward scan passive current density.
AW-105 Representative	Negative hysteresis, Category 1 (no pitting)	Negative hysteresis, Category 1 (no pitting)	Negative hysteresis, Category 1 (no pitting)	Mill-scale coupon's forward scan passive current density is 2-4 times lower than the bullet coupon's forward scan passive current density
AW-105 Elevated TOC	Negative hysteresis, Category 1 (no pitting)	Negative hysteresis, Category 1 (no pitting)	Negative hysteresis, Category 1 (no pitting)	Mill- and partial mill-scale coupons' forward scan passive current densities are one order of magnitude lower than the bullet coupon's forward scan passive current density

6.0 Conclusions

Conclusions for activities and experimental tasks that were performed for FY20 supporting Hanford DSTs are presented below in subsections.

6.1 New Limits Corrosion

An additional activity performed in FY19 that was not reported before, was added to provide a framework of nitrite concentration limits for inhibition towards localized corrosion, especially for dilute chemistries with pitting factors higher than 1.2. The test performed was Test 6 of the High Hydroxide Matrix from Hanford FY17 report. CPP showed a category 3 result and appearance of pits. By increasing nitrite from 0 M to 0.2 M, the PF increased from 1.95 to 2.02 and the CPP resulted in negative hysteresis with no pits, corresponding to a pass. This means that the addition of nitrite of just 0.2 M for this dilute chemistry was sufficient to prevent pitting corrosion. This data point, in conjunction with other data from the complete test matrix, was instrumental in establishing the minimum nitrite concentration to be 0.2 M.

6.2 Underdeposit Corrosion Testing

Modified AZ-101 simulant with pitting factor equal to two was used. The evaporated simulant salt was used as deposits. OLI simulations indicated that the salt deposits will include $NaF \cdot Na_2SO_4$ (Kogarkoite) that will persist and will not re-dissolve in the simulant. However, these deposits were not found to be adherent. As a result, the simulant chemistry above the deposits was able to percolate under the deposit and buffer any local chemistry under the deposits. This study indicated that presence of non-porous adherent deposits is needed to potentially initiate and propagate the underdeposit corrosion.

6.3 Secondary Liner Corrosion

VSC and immersion tests with commercially available VCIs were performed on the rail-road car carbon steel samples at specific concentrations mixed with the groundwater (GW) simulant. VCIs recommended dosages used for the study are:

- VCI-A: VpCI-337 – 10% v/v solution in GW simulant, i.e., 100 mL in VpCI-337 plus 900 mL of water for 1 L VCI formulation.
- VCI-B: 10% wt. VpCI-609 in GW simulant (100 g VpCI-609 in 1 liter) and 0.75% v/v VpCI-649MF (7.5 mL/L)

VCIs formulations were added during mid-course of experiments, i.e., after coupons had experienced corrosion in the untreated GW simulant. Three tests were conducted using VCI-A and VCI-B. The first two tests were conducted using 100% recommended dosages of VCI-A or VCI-B. The third test was conducted at 50% of the recommended dosage of VCI-B. Following conclusions are made from the experimental data and results:

- Both VCIs were effective in mitigating the pitting corrosion rate in immersed, Levels 1 and 2 coupons at the 100% recommended dosages. VCI-B was effective in mitigating the corrosion rate even at Level 3. VCI-A also mitigated the pitting corrosion rate in the Level 3 coupons, but statistical analysis of the corrosion rate data indicated that the corrosion rate reduction at best has a confidence of 91%, slightly below the 95% level.

- 100% VCI-B was also effective in mitigating the surface average corrosion rate in the immersed, Level 1, and Level 2 coupons with 95% confidence, whereas VCI-A was only effective in the

immersed coupons with 95% confidence. 50% VCI-B was also effective in mitigating the surface average corrosion rate in the immersed and Level 1 coupons with 95% confidence.

- 50% VCI-B was also effective in mitigating the pitting corrosion rate in immersed and Level 1 coupons with 95% confidence. The pitting corrosion rate was also mitigated at Levels 2 and 3 coupons, but the level of confidence was 92 and 91%, respectively, slightly below the 95% level.

6.4 <u>Long-term OCP Drift</u>

Evolution of the OCP was studied for three tank waste simulants identified as AY-101, SY-101, and AW-105 Base. In addition, two additional simulants based on AW-105 were studied: AW-105 with normal paraffin hydrocarbons (NPH) and small additions of tributyl phosphates (TBP) (i.e., AW-105 Representative) and AW-105 with NPH and larger additions of TBP (i.e., AW-105 Elevated TOC). Coupons with three different surface conditions were placed in each tank chemistry. The surface conditions included polished, mill-scale, and partial mill-scale. The corrosion potentials of the coupons with the three different conditions evolved to the same value in AY-101 simulant and appeared to reach a steady state. The OCP observations were mostly consistent with previous laboratory results. Anodic OCP drift was observed initially in all cases. In nearly all cases the final steady-state potential appears to be dependent on the free hydroxide concentration.

The steady state value was slightly more negative (-63 mV) than the initial potential measured by the reference electrode in Tank AY-101 (i.e., -77 mV vs. SCE). The coupons' corrosion potentials in SY-101 differed by as much as 250 mV and continued to evolve even after 4000 hours of exposure. At the completion of the test, the potential for the polished bullet coupon remained approximately 250 mV more positive than the initial potential measured by the reference electrode in Tank SY-101. The potential for the partial mill scale and complete mill scale coupons exposed to SY-101 was approximately the same as the initial actual tank potential. However, the decrease in the potential for both coupons that was observed over the last 1500 hours of the laboratory test remains unexplained.

The corrosion potentials of the coupons in AW-105 Base were in the range of -200 to -300 mV_{SCE} after 4000 hours of exposure. Similarly, corrosion potentials of the coupons in AW-105 Representative were also at -200 to -300 mV_{SCE} after 2100 hours of exposure. The corrosion potentials of the coupons in AW-105 Elevated TOC were in the range of -450 to -600 mV_{SCE} after 4000 hours of exposure. The laboratory corrosion potential for all three samples exposed to AW-105 Representative were within 30 mV of the initial tank potential data. The bullet and mill-scale coupons exposed to AW-105 Base were also closest to the initial tank potential data. However, the laboratory potentials for all samples that were exposed to AW-105 Elevated TOC were nearly 200 mV more negative than the initial tank potential. This case was the only one in which the final potential was not dictated by the free hydroxide concentration. This effect of the organics on the potential has been observed previously and may offer insight as to why tanks that have wastes with high organic content are less susceptible to corrosive attack.

The CPP data for the three coupon types in the simulants exhibited category one response, i.e., pitting corrosion of the tank steel is unlikely in the simulants. However, the passive current density of the mill-scale and partial mill-scale coupons was one-two orders of magnitude higher than the bullet coupons in all simulant chemistries; similar trends were observed in the EIS data of the three coupon types in the simulants. The low-frequency impedance of the mill-scale and partial mill-scale coupons were lower than the bullet coupons impedance. The EIS and CPP data are cross-consistent, i.e., evidence of bullet coupons' lower passive current density compared to mill-scale and partial mill-scale coupons in the CPP current is exhibited in form of higher impedances of the bullet coupons compared to the other two coupon types.

There are two plausible explanations for the higher passive current densities of the mill-scale and partial mill-scale coupons compared to the bullet coupons: (i) there are anodic reactions other than the metal dissolution reactions that occur on the mill-scale and partial mill-scale coupons leading to higher current densities during the forward scans of the CPP curves, and (ii) the passive film that develops on the polished surface could not be fully developed due to presence of mill-scale and corrosion products on the mill-scale and partial mill-scale coupons. These two hypotheses require further investigations.

6.5 <u>Recommendations</u>

Recommendations for follow-on work are summarized next. Some of these recommendations have been incorporated into a proposal for FY21 activities.

Underdeposit Corrosion

- ➢ Investigate formation of non-porous adherent deposits.
- ➢ Investigate underdeposit corrosion under the non-porous adherent deposits.

Secondary Liner

- ➢ Conduct a control experiment to establish and compare efficacy of the VCIs.
- ➢ Investigate migration rates of the VCIs.
- ➢ Explore alternative corrosion mitigation methods such as nitrogen blanketing.

OCP Drift

- ➢ Utilizing coupons with various surface conditions, perform various electrochemical tests in three waste tanks simulants adding LPR tests intermittently during the course of the test.
- ➢ Identify source(s) of corrosion potential drift and quantify extent of drift as a function of simulant chemistry and metal surface condition, and;
- ➢ Determine the effect of the potential drift on the interpretation of pitting corrosion data.

7.0 References

[1] B. J. Wiersma, R. E. Fuentes, L. Stock, Chemistry Envelope for Pitting and Stress Corrosion Cracking Mitigation", SRNL-STI-2019-00217, Savannah River National Laboratory, Aiken, September 2019.

[2] R. E. Fuentes, P. K. Shukla and B. J. Wiersma, "SRNL Task Technical and Quality Assurance Plan for Hanford Double Shell Waste Tank Corrosion Studies-FY2020", SRNL-RP-2020-00144, Savannah River National Laboratory, Aiken, SC, April 2020.

[3] R. E. Fuentes. B. J. Wiersma and K. Hicks, "Hanford Double Shell Waste Tank Corrosion Studies-Final Report FY14", SRNL-STI-2014-00616, Savannah River National Laboratory, Aiken, December 2014.

[4] R. E. Fuentes and R. B. Wyrwas, "Hanford Double Shell Waste Tank Corrosion Studies-Final Report FY15", SRNL-STI-2016-00117, Savannah River National Laboratory, Aiken, May 2016.

[5] R. E. Fuentes, "Hanford Double Shell Waste Tank Corrosion Studies-Final Report FY17", SRNL-STI-2018-00116, Savannah River National Laboratory, Aiken, April 2018.

[6] R. E. Fuentes, "Hanford Double Shell Waste Tank Corrosion Studies-Final Report FY16", SRNL-STI-2016-00721, Savannah River National Laboratory, Aiken, February 2017.

[7] R. E. Fuentes and P. K. Shukla, "Hanford Double Shell Waste Tank Corrosion Studies-Final Report FY2019", SRNL-STI-2020-00109, Savannah River National Laboratory, Aiken, July 2020.

[8] Best Basis Inventory, BBI Report RPP-RPT-44637, Rev. 12, Washington River Protection Solutions, October 2017.

[9] R. E. Fuentes, P. K. Shukla, B. Peters, D. A. Hitchcock, "Hanford Double Shell Waste Tank Corrosion Studies-Final Report FY2018", SRNL-STI-2019-00014, Savannah River National Laboratory, Aiken, August 2019.

[10] ASTM A515, "Standard Specification for Pressure Vessel Plates, Carbon Steel, for Intermediate- and Higher-Temperature Service", ASTM International, West Conshohocken, PA, 2003.

[11] ASTM G1-03 "Standard Practice for Preparing, Cleaning, and Evaluating Corrosion Test Specimens", ASTM International, West Conshohocken, PA, 2011.

[12] ASTM G5-13 "Standard Reference Test Method for Making Potentiodynamic Anodic Polarization Measurements", ASTM International, West Conshohocken, PA, 2013.

[13] T. Martin, "Outcomes from the August 2013 Expert Panel Oversight Committee Meeting," RPP-ASMT-56781, Washington River Protection Solutions LLC, Richland, WA, February 2014.

Appendix A Chemical Composition of Simulants used in Secondary Liner Corrosion Testing

Table A-1 Composition for GW simulant

Temperature	45	°C	
pH adjusted	7.6		
Volume	2	L	

Simulant Source	Formula	Concentration (M)	Weight required (g)
Sodium bicarbonate	$NaHCO_3$	1.750E-03	0.2940
Calcium hydroxide	$Ca(OH)_2$	1.500E-03	0.2223
Potassium nitrate	KNO_3	2.400E-04	0.0485
Ferric sulfate	$Fe_2(SO_4)_3$	6.250E-04	0.4999
Ferric chloride	$FeCl_3$	7.667E-05	0.0249
Strontium Nitrate	$Sr(NO_3)_2$	2.874E-06	0.0012
Sodium Metasilicate, 5-hydrate	$Na_2SiO_3.5H_2O$	6.000E-04	0.2546
Magnesium Chloride	$MgCl_2$	3.100E-04	0.0590
Acetic Acid	$C_2H_4O_2$	3.000E-04	0.0360

Appendix B Pictures of Secondary Liner Corrosion Testing Samples after Test

Samples cold mounted

Vessel 1: Level 3
2 months

6 months

Vessel 1: Level 2
2 months
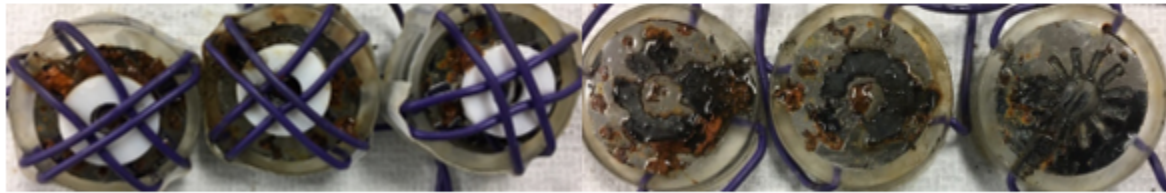
6 months

Samples cold mounted
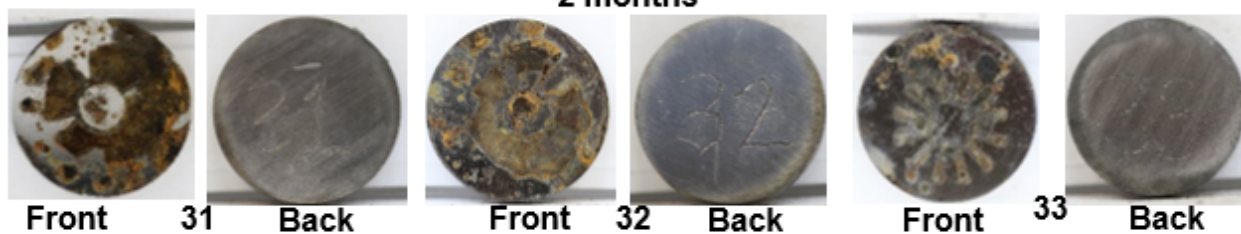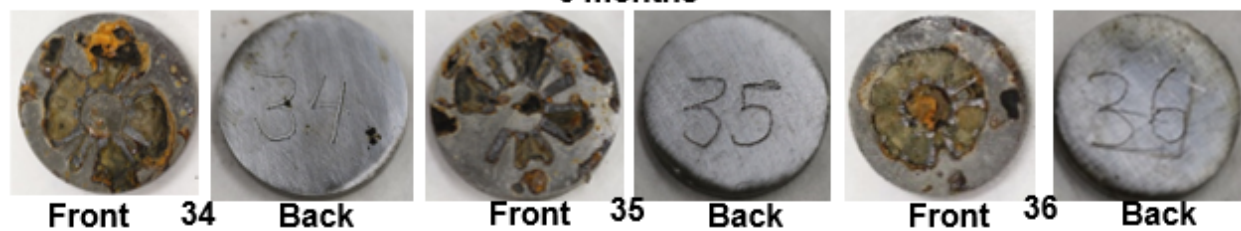
Vessel 1: Level 1
2 months
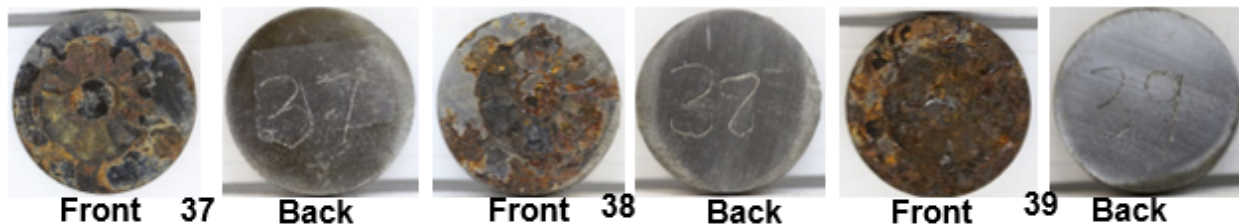
6 months

Vessel 1: Immersed
2 months

6 months

,

After removal of cold mount

Vessel 1: Level 3
2 months

Front 25 Back | Front 26 Back | Front 27 Back

6 months

Front 28 Back | Front 29 Back | Front 30 Back

Vessel 1: Level 2
2 months

Front 31 Back | Front 32 Back | Front 33 Back

6 months

Front 34 Back | Front 35 Back | Front 36 Back

After removal of cold mount

Vessel 1: Level 1
2 months

Front 37   Back   Front 38   Back   Front 39   Back

6 months

Front 40   Back   Front 41   Back   Front 42   Back

Vessel 1: Immersed
2 months

Front 43   Back   Front 44   Back   Front 45   Back

6 months

Front 46   Back   Front 47   Back   Front 48   Back

After cleaning with Clarke's solution

Vessel 1: Level 3
2 months

Front 25 Back   Front 26 Back   Front 27 Back

6 months

Front 28 Back   Front 29 Back   Front 30 Back

Vessel 1: Level 2
2 months

Front 31 Back   Front 32 Back   Front 33 Back

6 months

Front 34 Back   Front 35 Back   Front 36 Back

After cleaning with Clarke's solution

Vessel 1: Level 1
2 months

| Front | 37 | Back | Front | 38 | Back | Front | 39 | Back |

6 months

| Front | 40 | Back | Front | 41 | Back | Front | 42 | Back |

Vessel 1: Immersed
2 months

| Front | 43 | Back | Front | 44 | Back | Front | 45 | Back |

6 months

| Front | 46 | Back | Front | 47 | Back | Front | 48 | Back |

Samples cold mounted

Vessel 2: Level 3
2 months

6 months

Vessel 2: Level 2
2 months

6 months

Samples cold mounted
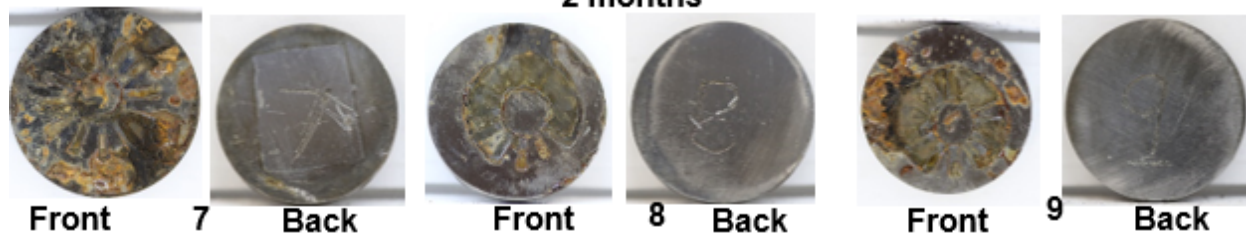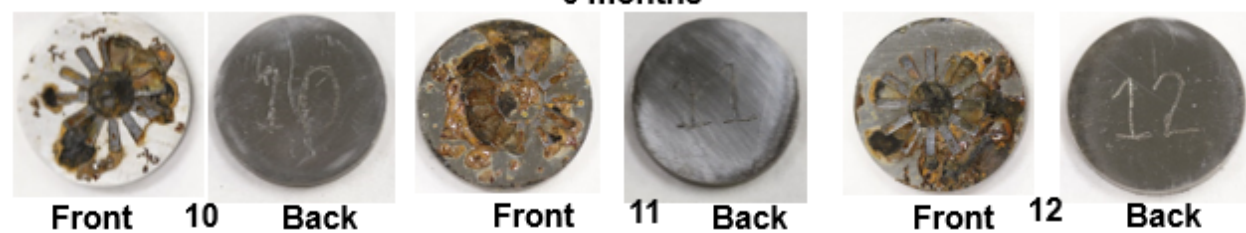
Vessel 2: Level 1
2 months
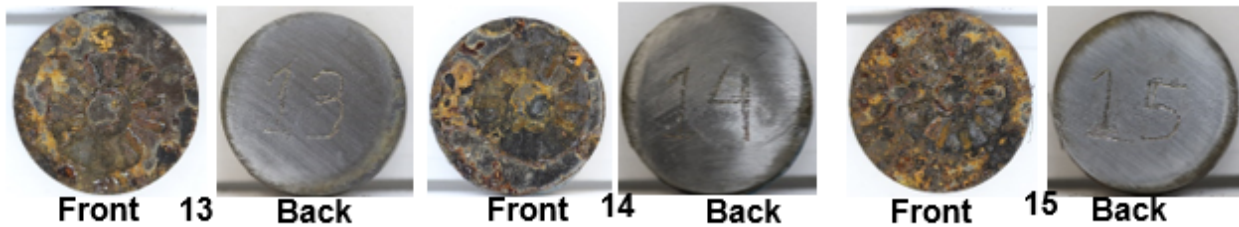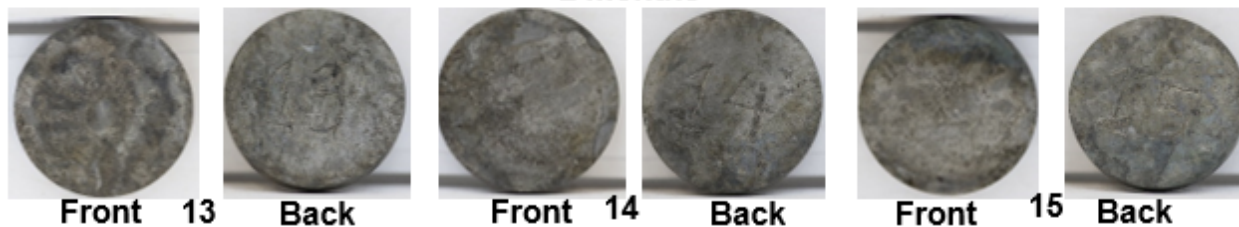
6 months

Vessel 2: Immersed
2 months

6 months

After removal of cold mount

Vessel 2: Level 3
2 months

Front   1   Back   Front   2   Back   Front   3   Back

6 months

Front   4   Back   Front   5   Back   Front   6   Back

Vessel 2: Level 2
2 months

Front   7   Back   Front   8   Back   Front   9   Back

6 months

Front   10   Back   Front   11   Back   Front   12   Back

After removal of cold mount

Vessel 2: Level 1
2 months

Front   13   Back   Front   14   Back   Front   15   Back

6 months

Front   16   Back   Front   17   Back   Front   18   Back

Vessel 2: Immersed
2 months

Front   19   Back   Front   20   Back   Front   21   Back

6 months

Front   22   Back   Front   23   Back   Front   24   Back

After cleaning with Clarke's solution

Vessel 2: Level 3
2 months

| Front | 1 | Back | Front | 2 | Back | Front | 3 | Back |

6 months

| Front | 4 | Back | Front | 5 | Back | Front | 6 | Back |

Vessel 2: Level 2
2 months

| Front | 7 | Back | Front | 8 | Back | Front | 9 | Back |

6 months

| Front | 10 | Back | Front | 11 | Back | Front | 12 | Back |

After cleaning with Clarke's solution

Vessel 2: Level 1
2 months

| Front 13 | Back | Front 14 | Back | Front 15 | Back |

6 months

| Front 16 | Back | Front 17 | Back | Front 18 | Back |

Vessel 2: Immersed
2 months

| Front 19 | Back | Front 20 | Back | Front 21 | Back |

6 months

| Front 22 | Back | Front 23 | Back | Front 24 | Back |

Samples cold mounted

Vessel 3: Level 3
2 months

6 months

Vessel 3: Level 2
2 months

6 months

Samples cold mounted
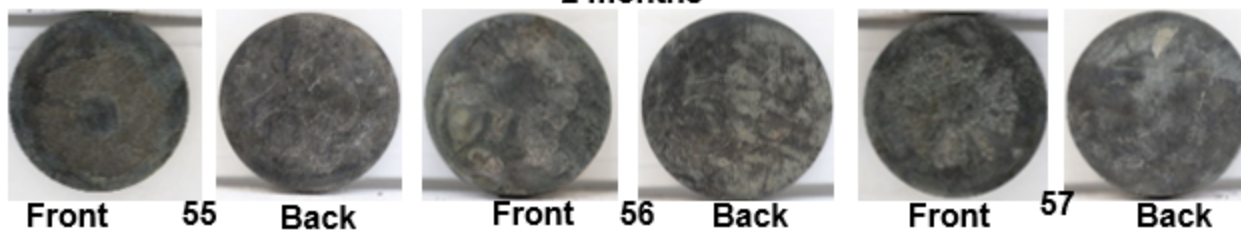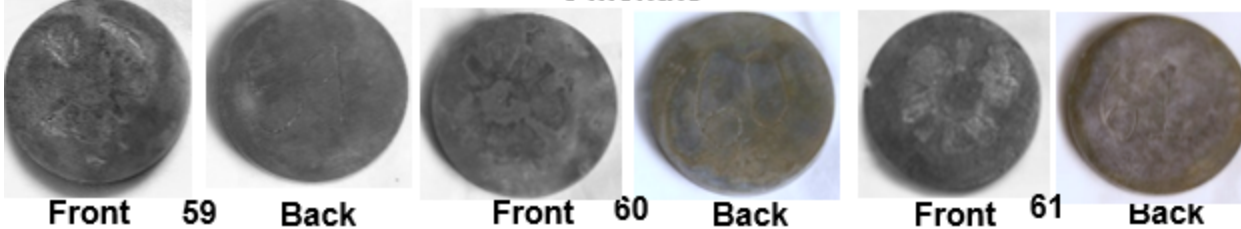
Vessel 3: Level 1
2 months
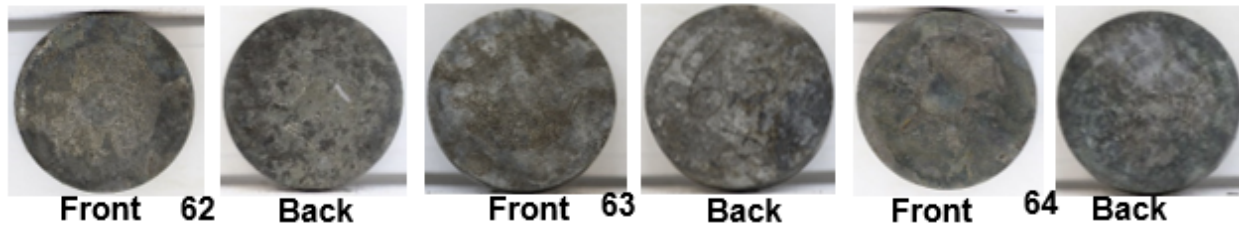
6 months

Vessel 3: Immersed
2 months

6 months

After removal of cold mount

Vessel 3: Level 3
2 months

Front 49 Back   Front 50 Back   Front 51 Back

6 months

Front 52 Back   Front 53 Back   Front 54 Back

Vessel 3: Level 2
2 months

Front 55 Back   Front 56 Back   Front 57 Back

6 months

Front 59 Back   Front 60 Back   Front 61 Back

After removal of cold mount

Vessel 3: Level 1
2 months

Front   62   Back   Front   63   Back   Front   64   Back

6 months

Front   65   Back   Front   67   Back   Front   68   Back

Vessel 3: Immersed
2 months

Front   70   Back   Front   71   Back   Front   72   Back

6 months

Front   73   Back   Front   74   Back   Front   75   Back

After cleaning with Clarke's solution

Vessel 3: Level 3
2 months

Front	49 Back	Front	50 Back	Front	51 Back

6 months

Front	52 Back	Front	53 Back	Front	54 Back

Vessel 3: Level 2
2 months

Front	55 Back	Front	56 Back	Front	57 Back

6 months

Front	59 Back	Front	60 Back	Front	61 Back

After cleaning with Clarke's solution

Vessel 3: Level 1
2 months

Front 62 Back Front 63 Back Front 64 Back

6 months

Front 65 Back Front 67 Back Front 68 Back

Vessel 3: Immersed
2 months

Front 70 Back Front 71 Back Front 72 Back

6 months

Front 73 Back Front 74 Back Front 75 Back
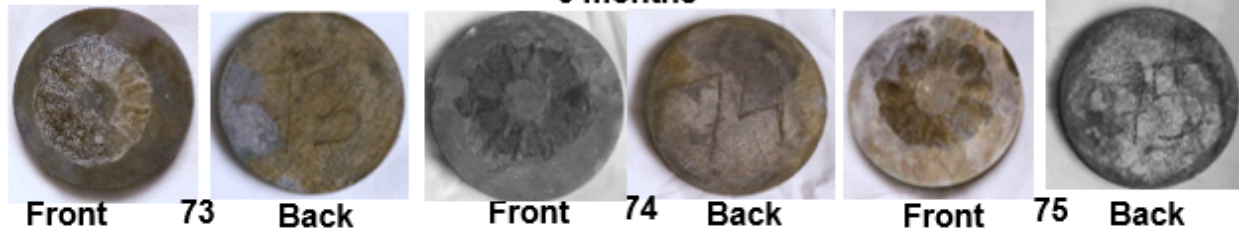
Distribution

alex.cozzi@srnl.doe.gov
Boyd.Wiedenman@srnl.doe.gov
Brenda.Garcia-Diaz@srnl.doe.gov
cj.bannochie@srnl.doe.gov
connie.herman@srnl.doe.gov
crystal_l_girardot@rl.gov
daniel.mccabe@srnl.doe.gov
Elaine_N_Diaz@orp.doe.gov
eric.skidmore@srnl.doe.gov
erik.nelson@rl.doe.gov
frank.pennebaker@srnl.doe.gov
Gregg.Morgan@srnl.doe.gov
jason_s_page@rl.gov
Joseph.Manna@srnl.doe.gov
Joshua.boerstler@srnl.doe.gov
michael.stone@srnl.doe.gov
Richard.wyrwas@srnl.doe.gov
robert_j_nelson@rl.gov
shawn_t_campbell@rl.gov
robert.sindelar@srnl.doe.gov
Andrew.duncan@srnl.doe.gov
Records Administration (EDWS)